



# LIBRARIES

UNIVERSITY OF WISCONSIN - MADISON

## **Groundwater modeling: semi-analytical approaches for heterogeneity and reaction networks.**

Lin Li; Benson, Craig H.

Madison, Wisconsin: University of Wisconsin Water Resources Institute, 2001-11-02

<https://digital.library.wisc.edu/1711.dl/UBIW7NIZKJWXX85>

<http://rightsstatements.org/vocab/InC/1.0/>

The libraries provide public access to a wide range of material, including online exhibits, digitized collections, archival finding aids, our catalog, online articles, and a growing range of materials in many media.

When possible, we provide rights information in catalog records, finding aids, and other metadata that accompanies collections or items. However, it is always the user's obligation to evaluate copyright and rights issues in light of their own use.

# GROUNDWATER MODELING: SEMI-ANALYTICAL APPROACHES FOR HETEROGENEITY AND REACTION NETWORKS

Lin Li, Gerald R. Eykholt, and Craig H. Benson

Geo Engineering Report No. 01-08

Geo Engineering Program  
Department of Civil and Environmental Engineering  
University of Wisconsin-Madison  
Madison, Wisconsin 53706

November 2, 2001

*This project was supported, in part, by General Purpose Revenue funds of the State of Wisconsin to the University of Wisconsin System for the performance of research on groundwater quality and quantity. Selection of projects was conducted on a competitive basis through a joint solicitation from the University and the Wisconsin Departments of Natural Resources; Agriculture, Trade and Consumer Protection; Commerce; and advice of the Wisconsin Groundwater Research Advisory Council and with the concurrence of the Wisconsin Groundwater Coordinating Council.*

## ABSTRACT

Reactive transport modeling for heterogeneous aquifers is challenging and computationally intensive. While numerical packages allow simulation of multiple species transport with aquifer heterogeneity, run times on high speed PCs and workstations make many jobs impractical. Stream tube approaches are computationally efficient numerical methods, and offer significant advantages in run time over more numerical methods.

In this study, a new stream tube model was developed for multiple species reactive transport in a heterogeneous aquifer. The model is based on a primary hypothesis that reactive transport in heterogeneous aquifers can be approximated with a linear transforms - where reactivity and flow distributions are not coupled. For many cases, the method allows good accuracy and significant computational advantages, especially for complex reaction networks and more heterogeneous aquifers.

The numerical experiments in this study have proved the hypothesis is correct. Comparisons are made between the new modeling approach, other analytical models and numerical models. Numerical agreements are reasonable for all of the tested cases, and significant computational time is saved with the new modeling approach. For a 2D aquifer simulation discussion in this study, the new approach is 1500 times faster than RT3D, one of the most popular numerical applications.

## **ACKNOWLEDGEMENTS**

Financial support for the research described in this report was provided by the State of Wisconsin Groundwater Coordinating Council (GCC), which is administered through the University of Wisconsin System Water Resources Institute. The findings and opinions expressed herein are those of the authors and are not necessarily consistent with the policies and opinions of the GCC. The authors would like to thank Prof. Mary Anderson and Dr. Carl Elder who assisted in developing the modeling strategy.

## TABLE OF CONTENTS

ABSTRACT.....	I
ACKNOWLEDGEMENTS.....	III
TABLE OF CONTENTS .....	IV
LIST OF FIGURES.....	VI
LIST OF TABLES .....	VIII
1. INTRODUCTION.....	1
2. BACKGROUND.....	3
2.1 HETEROGENEOUS AQUIFERS .....	3
2.2 REACTION NETWORKS .....	4
2.3 MODELING APPROACH.....	5
3. METHODS .....	9
3.1 OVERVIEW .....	9
3.2 AQUIFER SIMULATION .....	9
3.2 STEADY-STATE FLOW SIMULATION.....	13
3.2.1 <i>Governing equation</i> .....	13
3.2.2 <i>Problem Conceptualization</i> .....	13
3.3 RESIDENCE TIME DISTRIBUTION THEORY .....	14
3.3.1. <i>Overview</i> .....	14
3.3.2. <i>Residence time density function in simple systems</i> .....	16
3.3.3. <i>Residence time density function in complex systems</i> .....	18
3.3.4 <i>Numerical expression of residence time density function</i> .....	19
3.3.5 <i>Kinetic Response Function (KRF)</i> .....	23
3.3.6 <i>Kinetic Response Function Approach</i> .....	28
3.3.7 <i>RT3D</i> .....	28

4. RESULTS AND DISCUSSION .....	30
4.1. SIMPLE FLOW SYSTEM .....	30
4.2. COMPLEX FLOW SYSTEM .....	32
4.2.1. <i>Heterogeneous aquifer and numerical E-curve</i> .....	33
4.2.2. <i>Reactive transport simulation in heterogeneous aquifer</i> .....	40
4.3. SENSITIVITY ANALYSIS .....	46
4.3.1. <i>Mean of log-normal hydraulic conductivity</i> .....	46
4.3.2. <i>Standard deviation of log-normal hydraulic conductivity</i> .....	48
4.3.3. <i>Reaction parameters</i> .....	50
5. SUMMARY .....	51
REFERENCES.....	53

## LIST OF FIGURES

Figure 2-1 Example response function method simulation to model irreversible and reversible linear systems. ....	7
Figure 2-2 Comparison of kinetic response function method with Sun, <i>et al.</i> (1999) model analytical solution. ....	8
Figure 3-1 Kinetic response function modeling sequence scheme .....	11
Figure 3-3 Conceptual model of heterogeneous aquifer .....	14
Figure 3-4 Particle mass assigned as ratio of flow rate at the source.....	21
Figure 3-5 Particle tracking path from Path3D.....	21
Figure 3-6 Breakthrough curve at one location from MT3D result and corresponded numerical E curve from Eq. 3.18.....	24
Figure 3-7 Effective trajectory of a particle that degrades sequentially from species 1 to species 3. ....	26
Figure 3-8 Product and Kinetic Response Functions ( <i>PRF</i> and <i>KRF</i> ) for three species...	27
Figure 3-9 Steps for KRF approach used .....	29
Figure 4-1 Verification of kinetic residence time density method through comparison of CHAIN analytical solution (van Genuchten 1985). ....	31
Figure 4-2 Plume simulation at $t = 500$ d for 4 <sup>th</sup> species in a decay chain resulting from rectangular, continuous source of the 1 <sup>st</sup> species.....	32
Figure 4-3a Particle tracking path in a 2D heterogeneous aquifer.....	34
Figure 4-3b Numerical E-curve at receptor located at cell of column 90 and row 41. ....	35
Figure 4-4a Particle travel time in the hypothetical aquifer .....	36
Figure 4-4b Compared with MT3D in the hypothetical aquifer .....	36
Figure 4-5 Compared with MT3D in the heterogeneous aquifer.....	37
Figure 4-6a Tracer test along row 41 by MT3D in the heterogeneous aquifer. ....	38
Figure 4-6b Numerical E-curve along row 41 from MT3D tracer test. ....	39
Figure 4-7a Tracer test along column 80 by MT3D in the heterogeneous aquifer. ....	39
Figure 4-7b Numerical E-curve along column 80 from MT3D tracer test.....	40

Figure 4-8a Comparison of the four species concentration with KRF approach and RT3D at monitoring point (row 20, column 80).....	41
Figure 4-8b Comparison of the four species concentration with KRF approach and RT3D at monitoring point (row 45, column 80).....	42
Figure 4-8c Comparison of the four species concentration with KRF approach and RT3D at monitoring point (row 41, column 60).....	42
Figure 4-8d Comparison of the four species concentration with KRF approach and RT3D at monitoring point (row 41, column 100).....	43
Figure 4-9a Comparison of the four species concentration with KRF approach and RT3D at monitoring point (row 41, column 20).....	45
Figure 4-9b Comparison of the four species concentration with KRF approach and RT3D at monitoring point (row 41, column 40).....	45
Figure 4-9c Comparison of the four species concentration with KRF approach and RT3D at monitoring point (row 40, column 60).....	46
Figure 4-10a Numerical E curve under different mean of log-normal hydraulic conductivity at the row 41, and column 60. ....	47
Figure 4-10b RMS of the 4 <sup>th</sup> species between KRF model and RT3D model results under different mean of log-normal hydraulic conductivity.....	48
Figure 4-11a Numerical E curve under different standard deviation of log-normal hydraulic conductivity at the row 41, and column 80. ....	49
Figure 4-11b RMS of the 4 <sup>th</sup> species between KRF model and RT3D model results under different standard deviation of log-normal hydraulic conductivity.....	49



**LIST OF TABLES**

Table 3-1 Values of solution coefficient $G_{ij}$ used to express analytical solutions for PRF <sub>2</sub> and KRF <sub>3</sub> , for the cases with $R_1 \neq R_2$ , $R_2 \neq R_3$ and $R_1 \neq R_3$ .....	25
Table 4-1 Cases of heterogeneous aquifers in this study .....	33
Table 4-2 Comparison of run time between RT3D and KRF.....	44
Table 4-3 RMS difference in various reaction parameters.....	50

## 1. INTRODUCTION

Computer modeling is a necessary tool for the assessment of contaminant transport remediation designs, and long-term groundwater management. Some of the most challenging issues in the solute transport modeling include how to deal with aquifer heterogeneity of hydraulic conductivity and complex reaction networks.

The field of contaminant hydrogeology relies heavily on the numerical modeling packages, MODFLOW (MacDonald and Harbaugh 1988), MT3DMS (Zheng and Wang 1999), and RT3D (Clement 1997). MODFLOW is a three-dimensional groundwater flow simulator, based on the finite difference method. MT3DMS and RT3D rely on the head solution generated by MODFLOW. MT3DMS is used to simulate changes in concentrations of miscible contaminants in groundwater considering advection, dispersion, diffusion and some basic chemical reactions, with various types of boundary conditions and external sources or sinks. The basic chemical reactions included in the MT3DMS are equilibrium-controlled or rate-limited linear or non-linear sorption, and first-order irreversible or reversible kinetic reactions. MT3DMS is only for a single chemical species or compound. RT3D simulates multi-species reactive transport in saturated porous media. The model is capable of predicting the simultaneous, reactive fate and transport of multiple aqueous and solid-phase species.

The numerical models can be used for a wide range of problems, but are generally time-consuming. While computational power has advanced greatly in the last decade, the complexity and raw memory requirements of fate and transport problems have also increased. In addition, when modelers have more computational power, they often wish to simulate more complex problems that couldn't be modeled in the past. This project is proposed to develop, test, and explore new modeling strategies based on linear operator systems, in order to establish accurate and rapid simulations of contaminant fate and transport in heterogeneous aquifers with complex reaction networks. Our focus is on steady state flow and dissolved contaminants.

The objectives of this study include testing the performance of linear operator methods for simulation of first-order decay reactions in heterogeneous aquifers, and how to extend the solutions to assess how irregular sources and mixed-order kinetics processes affect the contaminant transport. Accuracy of the proposed numerical approach solutions and run times will be compared with RT3D and/or analytical solutions.

## 2. BACKGROUND

This section provides some background on important tools and proof of concept tests that are used to construct or test the new modeling method. In order to better address modeling in heterogeneous aquifers, a brief discussion is present of methods used to generate random fields for heterogeneous aquifer realizations. First order reaction networks concepts and multispecies transport are also discussed.

### 2.1 Heterogeneous Aquifers

Heterogeneous porous media are caused by complex geological processes which yield spatial variations in soil and rock properties. Aquifers are heterogeneous with respect to causing variations in flow magnitude and direction. Variations in chemical composition also cause heterogeneity, yielding different chemical reaction rates and sorption capacity. The uncertainty of chemical, biological, and physical heterogeneity is a primary challenge of exploring the hydrogeologic problems of water supply, remediation, and site selection for toxic and nuclear waste. It has been recognized that heterogeneity of chemical, biological, and flow conditions is often a major concern in many remediation scenarios.

Because of limited physical characteristics of field hydraulic conductivity, stochastic approaches are often used to create random fields of hydraulic conductivity based on field measurement (Anderson, 1997, Elder 2000). There are two common methods for generating three-dimensional, random fields that represent the distribution of hydraulic conductivity in an aquifer. One method is to use sedimentary models that distribute facies within a geologic region by considering the lithology and depositional history of a site (Webb and Anderson 1996). The other method is to use stochastic models that assume hydraulic conductivity is a second-order, stationary random field that is characterized by a mean and covariance function (Mantoglou and Wilson 1982). The sedimentary model of hydraulic conductivity often requires site data that may not be available. The second-order stochastic model multiplies normal random variable by the

standard deviation of the log-normal distribution for the hydraulic conductivity ( $\sigma_{\ln K}$ ), adding the mean of the hydraulic conductivity distribution ( $\mu_{\ln K}$ ), and transforming the random variable as hydraulic conductivity for each block using a natural logarithm function (Elder 2000). The advantage of the second approach is that only the mean and covariance structure for the simulated hydraulic conductivity fields are required, and it can produce large fields are readily available and well documented. A disadvantage of the second-order stochastic approach is that the model assumes that hydraulic conductivity across the problem domain can be described by only a mean and covariance.

The turning bands method (TBM) (Mantoglou and Wilson 1982, Tompson et al. 1989) is an efficient stochastic method for creating heterogeneous aquifers because it uses many spectral line processes that extend radially from a common origin within the domain to generate large, two- or three-dimensional, standard normal, random fields. The method involves projecting values from several spectral density line processes to discrete points in the random field. The random value at each point is then calculated as the weighed sum of inverted spectra that have been projected to the point from a finite number of spectral line processes (Mantoglou and Wilson 1982). The TBM method was modified and was used by Elder (2000) to demonstrate the effects of heterogeneity on reactive barrier performance. The aquifers simulated by Elder were shown to exhibit realistic geological structures and transport behavior that is consistent with actual aquifers. The TBM method was used in this project to create large, two- and three-dimensional heterogeneous aquifers that are input into MODFLOW. Path3D, MT3DMS, and RT3D use the MODFLOW head solutions and flow conditions to simulate particle movement and contaminant transport.

## **2.2 Reaction Networks**

When groundwater contaminants are degraded in the subsurface, there are always reaction by-products. For example, tetrachloroethene (PCE), one of most common chlorinated solvents contaminants in groundwater, yields less-chlorinated ethenes and other products via reductive dehalogenation under anaerobic conditions, or cometabolic

degradation under aerobic conditions. Biotransformation of the chlorinated ethenes often occurs via sequential, reductive dechlorination of PCE to TCE (trichloroethylene), TCE to DCE (dichloroethene), DCE to VC (vinyl chloride), and finally VC to ethene. However, under favorable environmental conditions, other abiotic and biochemical processes may also degrade the chlorinated organics. Sorption and dispersion of chlorinated species may also serve as natural attenuation processes. Due to differences in structure and sorption affinity for aquifer sediments, chlorinated species have different retardation coefficients. Reductive dechlorination is often modeled as a sequential, first-order decay process (Clement et al. 2000). This means that a parent compound undergoes first-order decay to produce a daughter product and that product undergoes first-order decay and so on. More complex reaction pathways involving elimination, inhibition, or metabolism may also be considered (Roberts, et al, 1996; Arnold and Robert, 1998).

In this study, chemical reactions with multiple sources and products are described mathematically as linear reaction networks (Eykholt 1999).

## **2.3 Modeling Approach**

Groundwater fate and transport modeling has advanced greatly over the last three decades. Innovative computational approaches and great advances in raw computational power have allowed scientists and engineers to model groundwater flow for heterogeneous aquifers and to simulate chemical fate and transport in the same aquifers. MODFLOW, Path3D, MT3DMS and RT3D have been tested rigorously, extended routinely, and are used widely in practice.

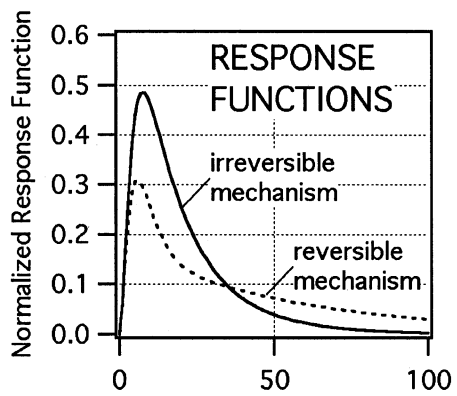
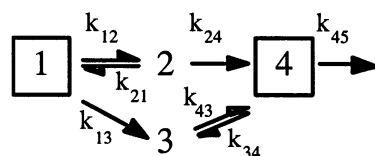
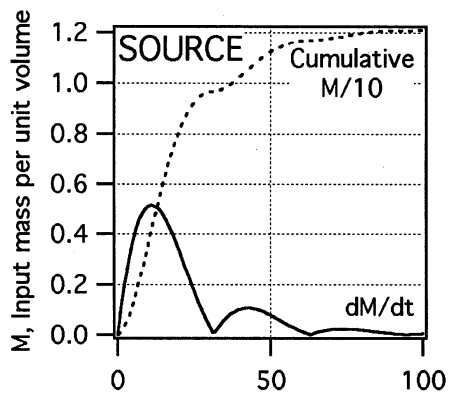
Still, a large set of modeling tasks are currently difficult to complete due to slow run times, especially for heterogeneous aquifers and complex reaction networks. For instance, RT3D was applied by us to solve contaminant transport in heterogeneous aquifers for the assessment of natural attenuation. For 480 m x 240 m aquifers, with 3 m grid spacing, RT3D simulations generally take 24 hours to complete on PC with Pentium

III 600MHz, 128M RAM. While great advances have come about from numerical groundwater contaminant transport models such as MT3DMS and RT3D, there is a significant motivation to test semi-analytical solutions as computationally efficient methods for groundwater contaminant transport modeling.

Other stream tube models (Jury 1982; Yabusaki *et al.* 1998; Cirpa and Kitanidis, 2000; Grin 2001) have also been developed. Often those stream tube approaches implement nonlinear transport (advection, dispersion, reaction) in each stream tube. However, these methods integrate overall response numerically - without advantage of the computation efficiency of linear operator methods.

A primary hypothesis of this work is that, for some problems, reactive transport in heterogeneous aquifers can be modeled with a linear method - where reactivity and flow distributions are not coupled (as in the nonlinear stream tube methods). If this is the case, then would be significant computational advantages, especially for complex reaction networks and heterogeneous aquifers. There are several important papers which provide tools used to develop and test the hypothesis. Eykholt (1999) includes a new solution form for first-order reaction and flow networks. A stochastic modeling framework (Eykholt, *et al.* 1999), based on stream tube modeling, demonstrated the effects of heterogeneity on reactive barrier performance. Eykholt and Lin (2000) developed a transfer function approach for decay chains with species having different retardation coefficients, named the kinetic response function (KRF) method. The semi-analytical approaches used in these studies lead to highly accurate and computationally efficient modeling methods.

An example is shown in Fig.2-1, for a four-member first-order reaction network. The solution is compared to a fourth-order Runge-Kutta integration method. This example shows that both irreversible and reversible systems with first-order kinetics can be modeled accurately with the KRF method.



First Order Decay Constants

	irreversible	reversible
k12	0.50	0.50
k13	0.20	0.20
k21	0.00	0.14
k24	0.35	0.35
k34	0.05	0.05
k43	0.00	0.13
k45	0.09	0.09

inverse time units

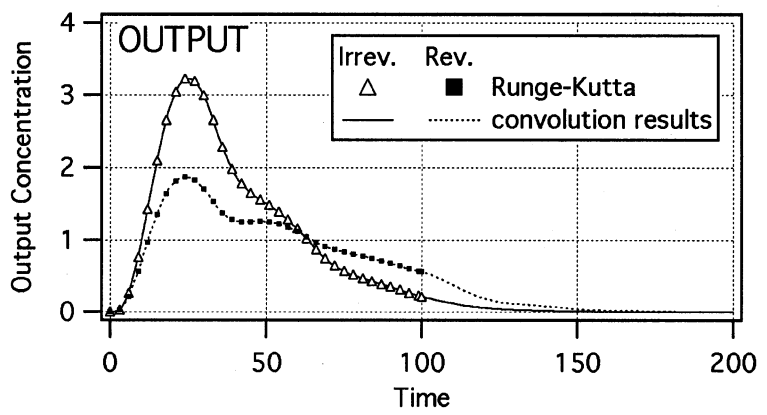


Figure 2-1 Example response function method simulation to model irreversible and reversible linear systems. (simulated response of fourth species in a first-order reaction network with irregular input of first species. Output functions computed with 4<sup>th</sup> order Runge-Kutta and convolution methods. Units on time and rate constant are arbitrary but consistent.)



In Fig.2-2, solutions from KRF approach are compared to analytical solutions for a straight decay-chain of four species with no retardation ( $R_i = 1$ ) and 1D advection-dispersion (Sun, *et al.* 1999). Solutions were found for a distance of  $L = 100$  m from the step-input point source and a constant velocity  $v = 0.2$  m/day. The set of first-order decay coefficients  $k_i$  was set to  $\{0.005, 0.02, 0.01, 0.0 \text{ day}^{-1}\}$ . A low dispersion coefficient ( $D$ ) or a high Peclet number ( $P = vL/D = 500$ ) was used. The agreement of the methods with regard to arrival time and species concentration is excellent. The maximum relative error at complete breakthrough is smaller than 0.03% for four species.

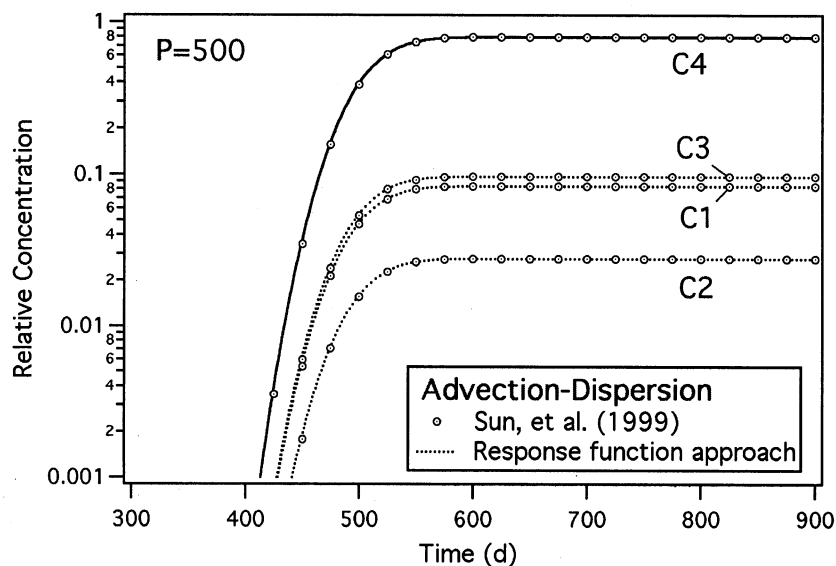


Figure 2-2 Comparison of kinetic response function method with Sun, *et al.* (1999) model analytical solution.

(Model run for  $R_i = 1$ ,  $k_i = \{0.005, 0.02, 0.01, 0.0 \text{ day}^{-1}\}$ , Peclet number  $P=500$ , and  $L/v = 500$  days.)

### 3. METHODS

This section explains the semi-analytical approach for modeling heterogeneity and reaction networks in this study. It includes four parts: (1) overview, (2) aquifer simulation, (3) steady-state flow simulation, (4) residence time distribution theory and the *Kinetic Response Function (KRF) approach*.

#### 3.1 Overview

Realistic, heterogeneous aquifers have been simulated through a stochastic, turning bands procedure (Tompson *et.al*, 1989, Elder, 2000). MODFLOW (MacDonald and Harbaugh, 1988) has been used to solve the head solutions and provide steady state flow for reactive transport. Using MODFLOW modeling runs, Path3D (Zheng 1991) or MT3D (1992) are modified to generate residence time distributions from a tracer source. Distributed and multiple point sources are considered and residence time distributions can be found through superposition. Convolution and other linear operator methods are used to generate responses from irregular source loadings, and to determine transient concentrations over the aquifer domain. Fig. 3-1 shows the general modeling sequence scheme used for this study.

#### 3.2 Aquifer Simulation

Aquifers that contain the range of hydraulic conductivity and geologic structure of natural aquifers can be created using a second-order stochastic, turning bands approach (Tompson *et.al*, 1989, Elder, 2000). This approach assumes that the hydraulic conductivity throughout the aquifer can be modeled as a correlated random field. The log-normal distribution is often used to describe the point distribution of hydraulic conductivity, and a correlation function is used to describe spatial correlation (Freeze 1975, Gelhar 1993, Fenton 1994).

The log-normal distribution for hydraulic conductivity is characterized by a mean  $\mu_{\ln K}$  and standard deviation  $\sigma_{\ln K}$  for the logarithm of hydraulic conductivity. The correlation

function is characterized by its functional form and the correlation lengths in principal directions ( $\lambda_x$ ,  $\lambda_y$ ,  $\lambda_z$ ). Aquifers with larger  $\mu_{\ln K}$  have higher hydraulic conductivity, aquifers with larger  $\sigma_{\ln K}$  have a greater range of hydraulic conductivity, and large  $\lambda$  corresponds to hydraulic conductivity that are more similar over greater distances.

The distribution of hydraulic conductivity in a three-dimensional heterogeneous aquifer was simulated using the turning band approach. Three-dimensional random fields were generated by stacked two-dimensional random fields by assuming vertical correlation lengths in aquifer less than vertical discretization chosen for the model (0.5 m). Two-dimensional Gaussian correlated random fields with  $\mu_{\ln K} = 0.2 \sim 1.8$  m/day,  $\sigma_{\ln K} = 0.2 \sim 2.0$ ,  $\lambda_x = 3 \text{m} \sim 9 \text{m}$ ,  $\lambda_y = 2 \text{m} \sim 8 \text{m}$  were generated. These properties are typical ranges from little to moderately heterogeneous sandy aquifer (Elder 2000). Cross section image of four example simulations are shown in Fig. 3-2.

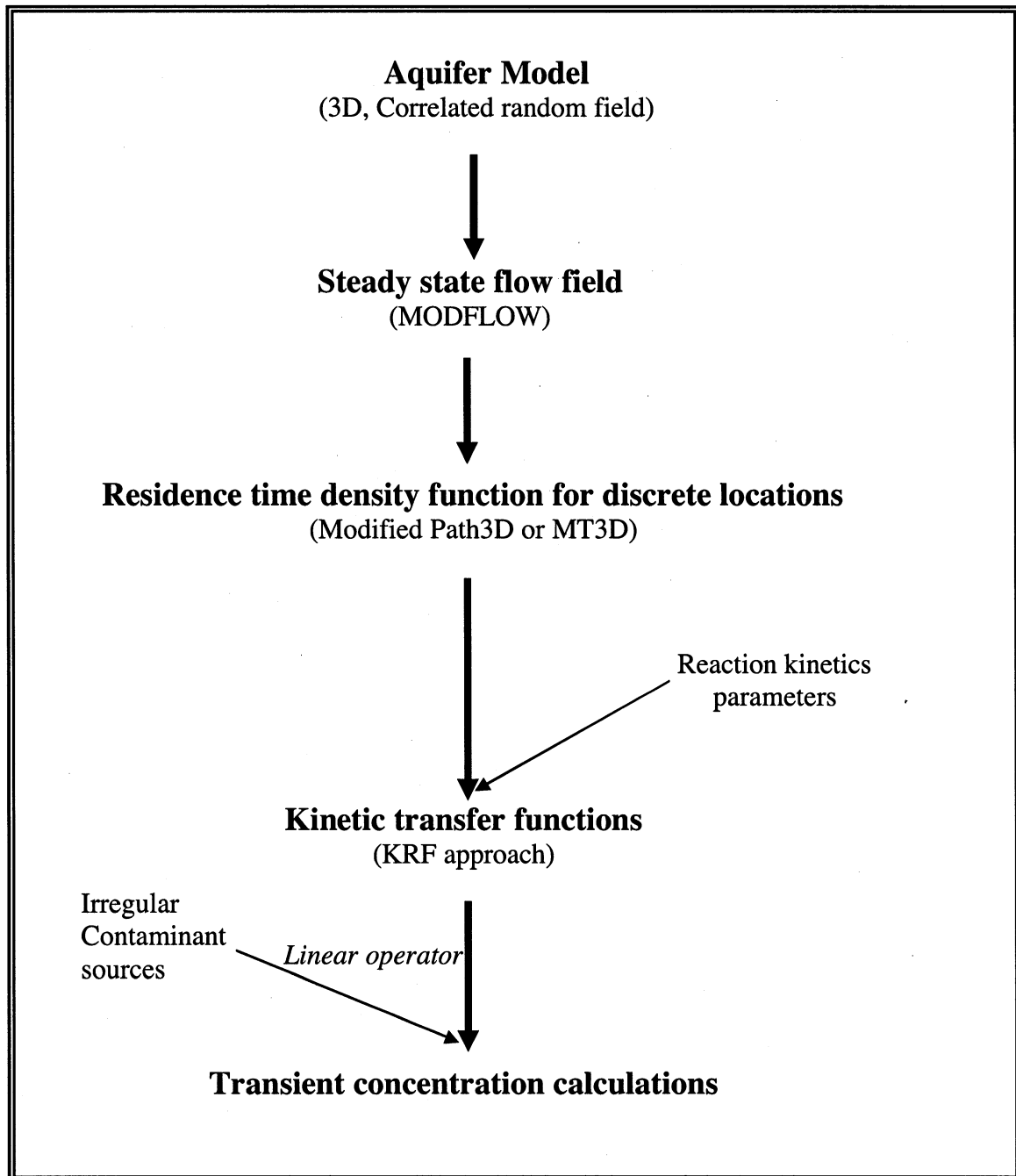


Figure 3-1 Kinetic response function modeling sequence scheme

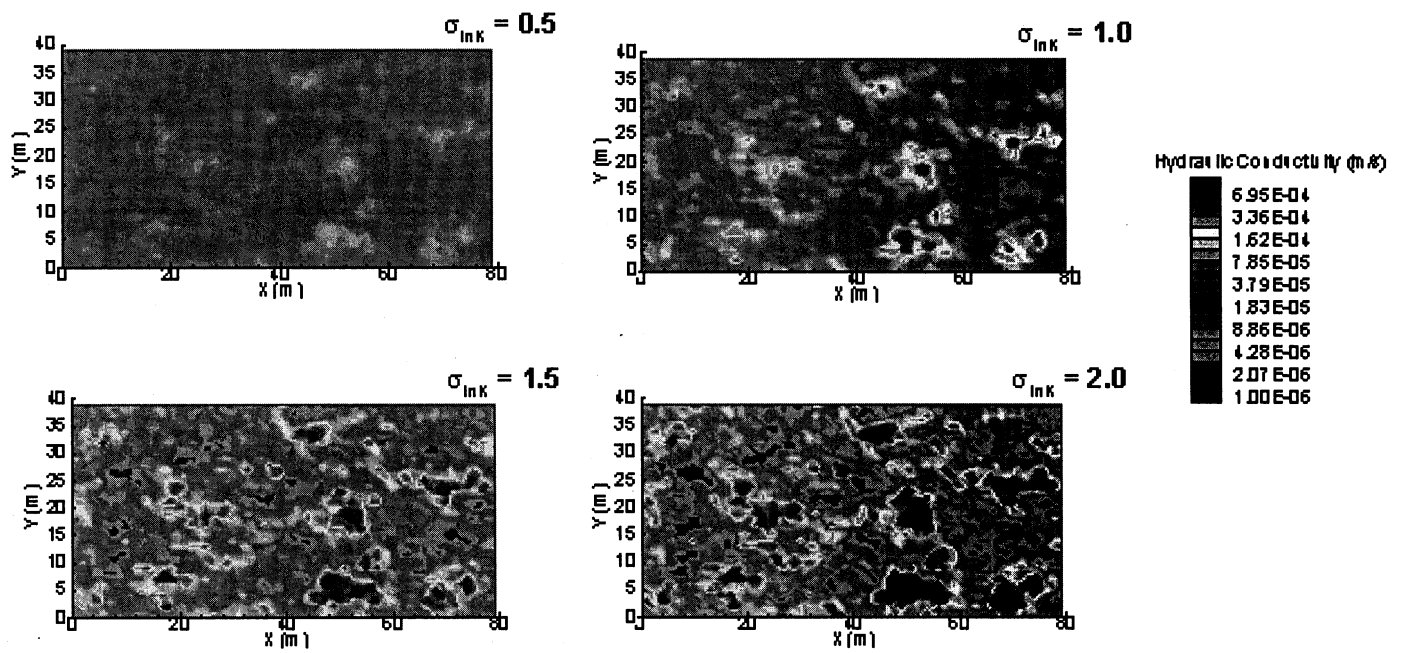


Figure 3-2 Heterogeneous hydraulic conductivity generated by turning band method.

## 3.2 Steady-State Flow Simulation

### 3.2.1 Governing equation

MODFLOW (McDonald and Harbaugh 1988) was used to compute the steady-state solution for head across heterogeneous aquifers. The head solution is obtained by solving the governing differential equation:

$$\frac{\partial}{\partial x} \left( K_{xx} \frac{\partial h}{\partial x} \right) + \frac{\partial}{\partial y} \left( K_{yy} \frac{\partial h}{\partial y} \right) + \frac{\partial}{\partial z} \left( K_{zz} \frac{\partial h}{\partial z} \right) - W = S_s \frac{\partial h}{\partial t} \quad (3.1)$$

where  $K_{xx}$ ,  $K_{yy}$ , and  $K_{zz}$  are hydraulic conductivities in orthogonal directions  $x$ ,  $y$ , and  $z$ ,  $h$  is total head,  $W$  is volumetric flux per unit volume for simulating sources and sinks,  $S_s$  is specific storage of the porous media, and  $t$  is time. Eq. 3.1 is solved by MODFLOW with corresponding boundary and initial conditions. For a steady-state simulation, the right-hand side of Eq. 3.1 is equal to zero (i.e., no change in aquifer storage) and initial conditions are not required.

### 3.2.2 Problem Conceptualization

The initial conceptual model of the problem is an unconfined (3D) or confined (2D) aquifer that is  $L_x$  long,  $L_y$  wide, and  $L_z$  thick, as shown in Fig. 3-3. The flow and heads are considered at steady state. Constant discretization was used for columns, rows and layers. Different hydraulic gradients were applied across the aquifer. Constant head boundary conditions were specified at the west and east faces to produce preferential groundwater flow from west to east. No flow boundary conditions were assigned to the north and south sides. In the three dimensional aquifer, the top layer was assigned as an unconfined layer, and the bottom layer was specified as a no flow boundary.

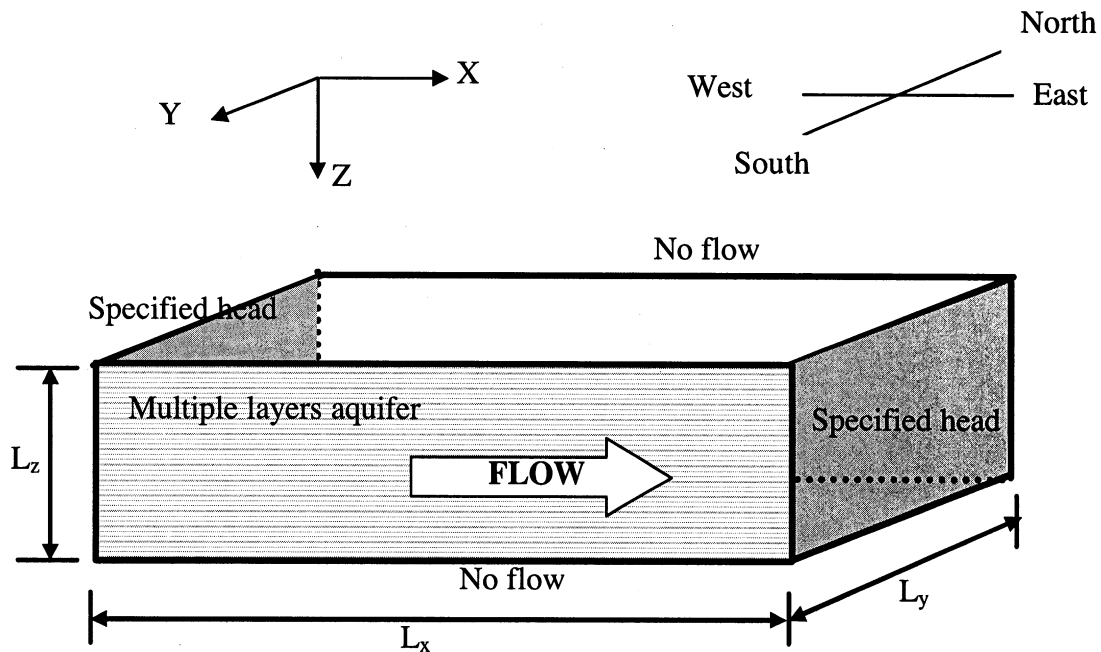


Figure 3-3 Conceptual model of heterogeneous aquifer

### 3.3 Residence Time Distribution Theory

#### 3.3.1. Overview

Under continuous, steady state flow, fluid elements in a flow system have an attribute other than compositional that can be used to characterize mixing. This attribute is called age, the time that a fluid element, Brownian particle or any conserved entity has spent in the system. Characterization of mixing in terms of ages allows a unified and elegant treatment of continuous flow system that is independent of specific mixing mechanisms. The treatment is called residence time theory.

Since the pioneering work of Danckwerts (1953), engineers and scientists have found that characterizing reactors in terms of residence time distribution is quite useful, such as in environmental engineering, chemical reaction engineering, electrical engineering, pharmacokinetics, acoustics, imaging (Nauman 1981). It avoids solving the detailed mixing characteristics in the flow system. With the residence time distribution from

pulse input measured at a monitoring point, response from any input loading to the reactor can be estimated with a convolution method. Solutions are exact for linear systems (i.e., first order reactions, completely stirred reactors), and nearly exact for many other systems. Levenspiel (1972) presents an excellent discussion of the residence time distribution theory for nonideal flow in chemical reactor design. Rainwater, *et al.* (1987), and Charbeneau (2000) have also used residence time theory for groundwater contaminant transport models.

A general mathematical description of the residence time distribution theory for a continuous flow reactor with irregular inputs, nonideal mixing, and first-order reaction networks with multiple chemical component is as follows (Eykholt and Lin 2000):

$$\dot{M}_{j,out}(t) = \dot{M}_{i,in}(t) * E(t) \cdot KRF_j(t) = \dot{M}_{i,in}(t) * E'_j(t) \quad (3.2)$$

where  $\dot{M}_{j,out}$  refers to the mass output rate expected from a nonuniform input of species  $i$  in the reactor. The symbol  $*$  represents the linear convolution operator.  $E'_j(t)$  is a reduced residence time distribution function for the amount of species  $j$  remaining at the output location from a unit input of the species. This function can be called the kinetic residence time distribution density, or the kinetic *E-curve*. The kinetic response function,  $KRF_j(t)$ , is the response of species  $j$  to an unit input of species  $i$  in a plug flow system due to reaction in a linear network. The KRF function can be expressed as analytical form (Eykholt and Lin 2000), and it will be discussed further below. The residence time density function  $E(t)$  is considered to be fixed in space and is easily interpreted for point-to-point mass transfer. Also, the Eq.3.2 includes different retardation coefficient effect in the reactive transport simulation. For N-CSTRs or a one dimensional advection-dispersion system with uniform flow, Eq.3.2 has been shown to be accurate (Eykholt and Lin 2000).

As stated above, the primary hypothesis of this work is that, for some problems, reactive transport in heterogeneous aquifers can be modeled with a linear method - where reactivity and flow distributions are not coupled. Eq.3.2 describes the stream tube



approach for the multiple species reactive transport in heterogeneous aquifers. If the residence time distribution  $E(t)$  of the system can be given, and the kinetic response function of each species is described, the fate and transport prediction of species concentration is straightforward. Here, the system  $E(t)$  is assumed to be independent on the kinetic response function KRF of each species, i.e., the flow distributions and reactivity are not coupled in the heterogeneous aquifer. In the following section, the residence time density  $E(t)$  in simple system and complex system will be expressed as analytical form or numerical form. The KRF function of each species will be discussed. With the system  $E(t)$  and each species KRF, multiple species reactive transport can be predicted for any non-ideal input via convolution.

### 3.3.2. Residence time density function in simple systems

#### 3.3.2.1. For steady flow and conservative particle

Often residence time distribution theory is discussed in terms of closed reactors with one input and one output. Here, a more general approach is needed. In a continuous, steady state flow system with one or more entrances and exits, conservative particles enter the control volume, remain in it for some period of time which may be either deterministic or probabilistic, and eventually leave. The age of a particle from first entrance to last exit from the system is called the residence time  $t$ . The residence time density function  $E(t)$  at the monitoring point satisfies:

$$\dot{M}_{out} = \dot{M}_{in} * E(t) \quad (3.3)$$

Where,  $\dot{M}_{out}$  is the rate of mass output,  $\dot{M}_{in}$  is the rate of mass input to the input plane. For steady flow and conservative tracers, the mass rate of output at an output receptor is equal to the mass rate of input convolved with the residence time density function  $E(t)$ , provided the system behaves linearly.

#### 3.3.2.2. For a pulse input

For a pulse input, the mass input rate is

$$\dot{M}_{in} = M_0 \delta(t) \quad (3.4)$$

where  $\delta(t)$  is the Dirac delta function, and  $M_0$  is the released mass at time zero. Substituting Eq.3.4 into Eq.3.3,

$$\dot{M}_{out} = M_0 \delta(t) * E(t) \quad (3.5)$$

For a pulse input, the residence time density function  $E(t)$  can be defined as

$$E(t) = \frac{\dot{M}_{out}}{M_0} \quad (3.6)$$

### 3.3.2.3. For one input and one output (CSTR)

For continuous flow systems,  $\dot{M}_{out}$  is equal to the product of the volumetric flow rate  $Q_{out}$  and the concentration of the conservative tracer at the monitoring point,  $C_{out}(t)$ . In a completely stirred tank reactor (CSTR),

$$\dot{M}_{out} = QC(t) \quad (3.7)$$

where,  $Q$  is flow rate,  $C(t)$  is concentration in the CSTR. Because of properties of CSTR, the  $C(t)$  is equal to  $C_{out}(t)$ , and  $Q(t)$  is same as  $Q_{out}$  for the steady flow and flow balance. The residence time density function  $E(t)$  for the CSTR under pulse input is

$$E(t) = \frac{QC(t)}{M_0} \quad (3.8)$$

Further,  $M_0 = C_0/V$ , where  $C_0$  is the concentration in the reactor immediately after the input at time zero and  $V$  is reactor volume, let residence time  $\theta = V/Q$ , so,

$$E(t) = \frac{C(t)}{\theta C_0} = \frac{C_0 e^{-t/\theta}}{\theta C_0} = \frac{e^{-t/\theta}}{\theta} \quad (3.9)$$

### 3.3.2.4. For advection-dispersion with uniform flow rate

For the advection-dispersion equation, 1<sup>st</sup> type boundary condition, the residence time density function at the output is (Eykholt and Lin 2000):

$$E(T) = \frac{\sqrt{RR}}{2\sqrt{P}} T^{-3/2} \exp\left(-\frac{R(R-T)^2}{4RT}\right) \quad (3.10)$$

Where, the dimensionless variable  $T$  is time,  $R$  is retardation coefficient,  $P$  is Peclet number.

For the one-dimensional flow, three-dimensional dispersion with a constant, rectangular, plane sources with dimensions of  $Y_0$  (width) and  $Z_0$  (depth), the analytical E-curve results from the time derivative of the conservative case (no decay):

$$E(x,y,z,t) = \frac{1}{16} \frac{x+vt}{\sqrt{\pi D_x} t^{3/2}} \exp\left\{-\frac{(x-vt)^2}{4(D_x t)}\right\} \left\{ \operatorname{erf} \frac{y+Y_0/2}{2(D_y x/v)^{1/2}} - \operatorname{erf} \frac{y-Y_0/2}{2(D_y x/v)^{1/2}} \right\} \left\{ \operatorname{erf} \frac{z+Z_0/2}{2(D_z x/v)^{1/2}} - \operatorname{erf} \frac{z-Z_0/2}{2(D_z x/v)^{1/2}} \right\} \quad (3.11)$$

Where  $D_x, D_y, D_z$  are the dispersion coefficients.  $v$  is uniform velocity along  $x$  direction.  $\operatorname{erf}()$  is error function.

### 3.3.2.5. For nonideal reactors

Eq.3.9 only define the residence time density function for CSTR under pulse input. For nonideal reactors, Eq.3.6 describe the  $E(t)$  under pulse input. For nonlinear input, convolution can be employed to predict output response to the linear reaction system as Eq.3.3. Superposition can be employed to calculate system output from multiple input response based on linearity. The  $E(t)$  can be analytical expressed in a simple system, such as CSTR or the uniform flow advection-dispersion case. For complex systems,  $E(t)$  maybe described with a numerical expression.

### 3.3.3. Residence time density function in complex systems

For complex systems, the residence time density function  $E(t)$  was determined by a numerical method, assuming a continuous flow reactor with a pulse input or continuous inputs. Path3D, one of particle tracking code, was modified to generate numerical  $E(t)$  at the monitoring point. Because of pure advective property of the Path3D, it is only used

in the case of pure advection flow. MT3D, a solute transport modeling code, provided a numerical tracer test to generate a numerical  $E(t)$  for the advection and dispersion flow system.

### 3.3.4 Numerical expression of residence time density function

#### 3.3.4.1. Introduction to Path3D

Path3D (Zheng 1992) is a computer program designed to run in series with MODFLOW and to simulate the movement of particles through the model domain. Path3D reads the head solution from MODFLOW and calculates the seepage velocity between cells of the model domain by linear interpolation, and then uses a fourth-order Runge-Kutta method to calculate the position of particles at time-steps. The movement of each particle across the aquifer is calculated discretely, and the duration of a time-step is controlled via an error criterion. Path3D reports the coordinates and seepage velocity of each particle at specified increments of time. Path3D assumes that gravitational forces do not influence the movement of particles and does not account for diffusion. The trajectory of particles through the domain is a result of advection and mechanical mixing caused by aquifer heterogeneity (Elder 2000). Usually, Path3D is used to visualize flow paths and to track contaminant paths. In this study, Path3D was modified to generate residence time density functions at specified locations in the model domain.

#### 3.3.4.2. Numerical $E(t)$ from Path3D

The residence time density function  $E(t)$  at a monitoring point can be determined numerically by conservative particle tracking results from modified Path3D. A continuous, steady state flow system is assumed. Pulse inputs are considered at the upstream sources, and each finite element of a source cell has been allocated mass in proportion to the ratio of flow rate (Fig.3-4):

$$M_{o,i} = \frac{Q_{in,i}}{\sum Q_{in,i}} M_{o,total} \quad (3.12)$$

Where  $M_{o,total}$  is total pulse input mass to the source,  $Q_{in,i}$  is flow rate of each source element. With steady state flow, the flow rate to the source elements is independent to the time. So, the mass rate to each source element is also independent of time.

The preferred strategy for Path3D is to release a fixed number of particles that are evenly or randomly distributed over the source cells. The total particle mass over each source cell is equal to sum of each particle mass in the cell. Assuming each particle in the source cell has same particle mass, each particle mass was assigned as:

$$m_i = \frac{M_{\text{each source element}}}{\text{number of particles in the source element}} \quad (3.13)$$

The mass at the source cell is also equal to assigned mass  $M_{o,i}$  from flow rate ratio, as described in Eq.3.12.

After each particle is released from the source, it moves with flow to a downstream position. In the advection-dominated flow, each particle is assumed to maintain mass  $m_i$  along its path. Particles from different source elements have different masses (Eq.3.12~Eq.3.13). At the monitoring point, the residence time density function  $E(t)$  determined from a pulse input can be described as:

$$E(t) = \frac{\dot{M}}{M_{o,total}} = \frac{\sum m_i \delta(t - \tau)}{M_{o,total}} \quad (3.14)$$

Where  $\dot{M}$  is the rate of mass output to the monitoring point as a response to a pulse input of mass  $M_{o,total}$  at the source. For the monitoring point,  $\dot{M}$  is equal to sum of passing particle mass rate  $\dot{m}$ . Each passing particle mass rate  $\dot{m}$  is particle mass multiplied by dirac delta function at the arrival time. Here,  $\delta(t)$  is dirac function,  $t$  is the particle travel time from the source,  $\tau$  is the particle arrival time in the monitoring point. Fig.3-5 shows particle tracking path from Path3D and define density function at the target cell or monitoring point.

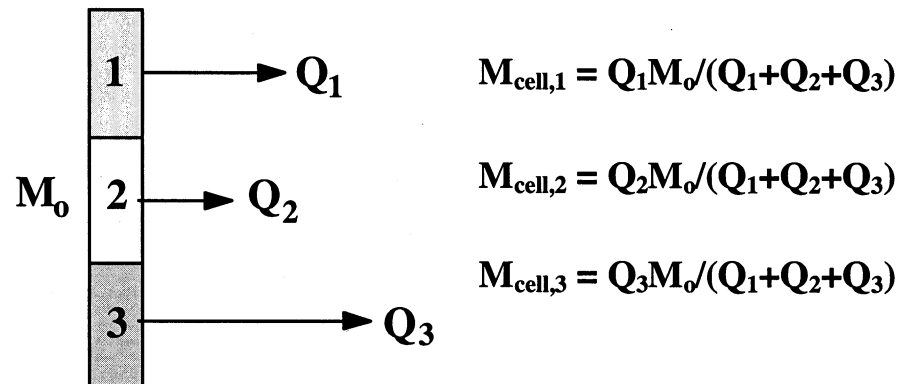


Figure 3-4 Particle mass assigned as ratio of flow rate at the source

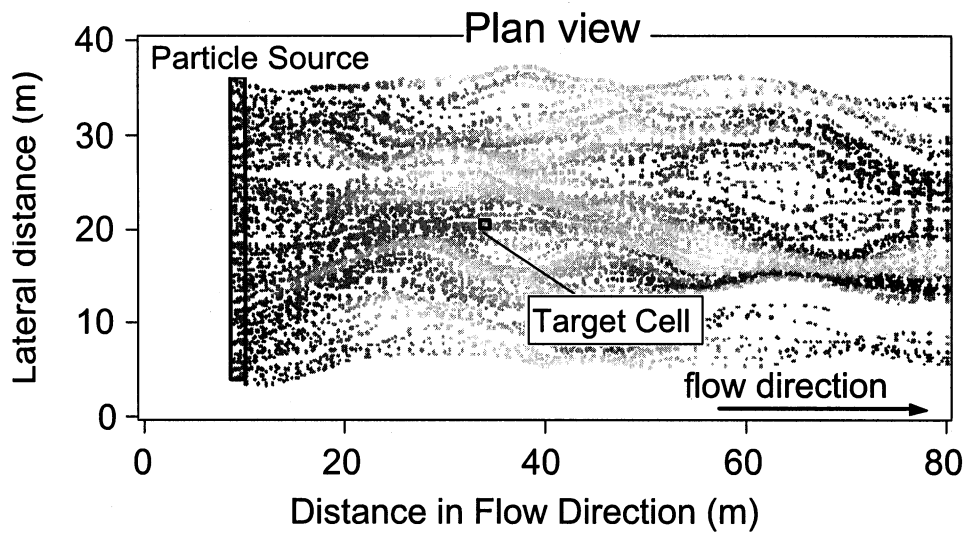


Figure 3-5 Particle tracking path from Path3D

#### 3.3.4.3. Introduction to MT3D

MT3D is a three-dimensional conservative solute transport model for simulation of advection, dispersion and chemical reactions of contaminants in groundwater systems. MT3D interfaces directly with MODFLOW for the head solution. The MT3D code uses

solver including the method of characteristics (MOC), the modified method of characteristics (MMOC), a hybrid of these two methods (HMOC), and the standard finite-difference method (FDM). It is usually used for risk assessment, parameter estimation, and remediation design optimization.

#### 3.3.4.4. Numerical $E(t)$ from MT3D

From the residence time distribution theory, the cumulative residence time distribution  $F(t)$  is (Danckwerts 1953, Nauman 1981)

$$F(t) = \int_0^t E(t') dt' \quad (3.15)$$

For a step input, the  $F(t)$  can also be defined as:

$$F(t) = \frac{\dot{M}_{out}(t)}{\dot{M}_{in}} \quad (3.16)$$

If continuous flow,

$$F(t) = \frac{Q_{out} C_{out}(t)}{\sum (Q_{in} C_{in})}$$

Where,  $\dot{M}_{out}$  is the rate of mass output to the monitoring point as a response to a step input of mass rate  $\dot{M}_{in}$  at the source.  $Q_{out}$  is flow rate at the monitoring point,  $Q_{in}$  is flow rate at the each source element.  $C_{out}(t)$  is output concentration at the monitoring point, and  $C_{in}$  is the steady input concentration at the source.

Conservative tracer tests were conducted with MT3D for heterogeneous aquifers. A continuous input with constant source concentration was assumed at the upper boundary, and a monitoring well was located within the downstream region. The breakthrough curve  $C(t)/C_0$  at each monitored well was recorded. For the continuous input in the tracer test, each breakthrough curve follows the trend of Ogata and Banks solutions in Eq.3.17 (Ogata and Banks 1961). By fitting the O&B solution (with  $R=1$ ), the  $E(t)$  can be defined analytically to give a smooth curve as shown in Eq. 3.18.

$$C(x, t) = \frac{C_o}{2} \left\{ \operatorname{erfc} \left( \frac{x - vt/R}{2\sqrt{Dt/R}} \right) + \exp \left( \frac{vx}{D} \right) \operatorname{erfc} \left( \frac{x + vt/R}{2\sqrt{Dt/R}} \right) \right\} \quad (3.17)$$

$$E(x, t) = \frac{x + vt/R}{4t\sqrt{\pi Dt/R}} \exp \left( -\frac{(x - vt/R)^2}{4Dt/R} \right) + \frac{x - vt/R}{4t\sqrt{\pi Dt/R}} \exp \left( \frac{vx}{D} \right) \exp \left( -\frac{(x + vt/R)^2}{4Dt/R} \right) \quad (3.18)$$

Where,  $C(x,t)$  is tracer concentration,  $C_o$  is source concentration,  $x$  is downstream distance from source,  $v$  is velocity along the main flow direction,  $t$  is time,  $R$  is retardation coefficient (fixed  $R=1$  for fitting).  $D$  is the dispersion coefficient.

Fig. 3-6 shows one simulation of MT3D in a 2D heterogeneous aquifer tracer test results. Only one monitoring well are listed and corresponded numerical E curve was simulated with Eq. 3.18.

### 3.3.5 Kinetic Response Function (KRF)

The kinetic response function reflects system response of reaction, including chemical reaction and sorption reaction to the unit input. The detailed concept can be referred in Eykholt and Lin (2000). For a three species sequential decay reactions with different retardation coefficient (Fig.3-7), the KRF of each species is analytically expressed as following:

$$\operatorname{KRF}_i(x, T) = \delta(x - T/R_i) e^{-\kappa_i x R_i} \quad (3.19)$$

Where,  $\kappa_i = \sum_j k_{ij}/R_i$  as a lumped loss rate coefficients, the dimensionless rate constant

$k_{ij}$  refers to the decay of species  $i$  to product species  $j$ , and  $R_i$  is retardation coefficient for species  $i$ .



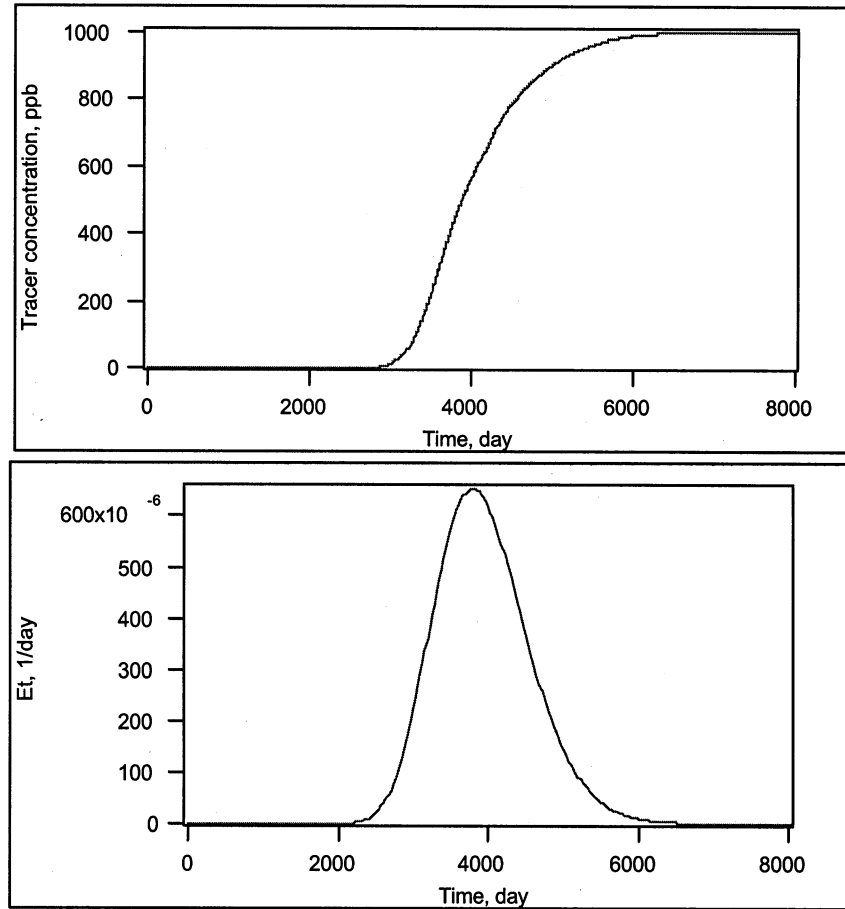


Figure 3-6 Breakthrough curve at one location from MT3D result and corresponded numerical E curve from Eq. 3.18

$$KRF_2(x, T) = \frac{k_{12}}{|R_1 - R_2|} \exp(-\kappa_1 \xi_{12} - \kappa_2 \xi_{21}) dT \quad (3.20)$$

$$(xR_1 \geq T > xR_2 \text{ or } xR_1 \leq T < xR_2)$$

$$\text{Where, } \xi_{ij} = \frac{R_i(T - R_j x)}{R_i - R_j}$$

$$\begin{aligned} \text{KRF}_3(x, T) = \alpha_3 & \left[ G_{12} \exp(-\kappa_1 \xi_{12} - \kappa_2 \xi_{21}) + G_{23} \exp(-\kappa_2 \xi_{23} - \kappa_3 \xi_{32}) \right. \\ & \left. + G_{31} \exp(-\kappa_3 \xi_{31} - \kappa_1 \xi_{13}) \right] dT \end{aligned} \quad (3.21)$$

$$\text{Where, } a_3 = \frac{k_{12} k_{23}}{k_1 R_1 (R_2 - R_3) + k_2 R_2 (R_3 - R_1) + k_3 R_3 (R_1 - R_2)}$$

The values for the coefficients  $G_{ij}$  can be -1, 1, or 0, and depend on the order of retardation coefficients. The coefficient values for all relevant cases are shown in Table 3-1. The minimum, middle, and maximum retardation coefficients are referred to as  $R_{min}$ ,  $R_{mid}$ , and  $R_{max}$ .

**Table 3-1 Values of solution coefficient  $G_{ij}$  used to express analytical solutions for  $\text{PRF}_2$  and  $\text{KRF}_3$ , for the cases with  $R_1 \pi R_2$ ,  $R_2 \pi R_3$  and  $R_1 \pi R_3$ .**

Case	$R_{min} < T/x \leq R_{mid}$			$R_{mid} < T/x \leq R_{max}$		
	$G_{12}$	$G_{23}$	$G_{31}$	$G_{12}$	$G_{23}$	$G_{31}$
$R_1 < R_2 < R_3$	-1	0	1	0	-1	1
$R_1 < R_3 < R_2$	-1	0	1	-1	1	0
$R_2 < R_1 < R_3$	1	-1	0	0	-1	1
$R_2 < R_3 < R_1$	1	-1	0	1	0	-1
$R_3 < R_1 < R_2$	0	1	-1	-1	1	0
$R_3 < R_2 < R_1$	0	1	-1	1	0	-1

A set of analytical solutions for the response functions of the first three species is shown in Fig. 3-8. Each solution set is shown to be symmetrical with one other case. With greater differences in the reactivity of the species, the functions can be quite sharp. For instance, if  $k_1 \gg k_2$ , the  $\text{KRF}_2$  will have a peak at  $T = R_2$ , with a sharp, exponential descent to zero. In effect, the function responds like a Dirac function, as if species 1 is immediately converted to species 2.

For 4 species in reactions network, there are developed KRF in Eykholt and Lin (2000) paper. If more than 4 species in the reactions network, KRF analytical expressions have not been developed. However, new solutions can be developed with the same logic used to develop solutions for smaller reaction networks. If all the species have the same retardation coefficient, the responds function for many species are easily obtainable from batch systems kinetics (Eykholt 1999).

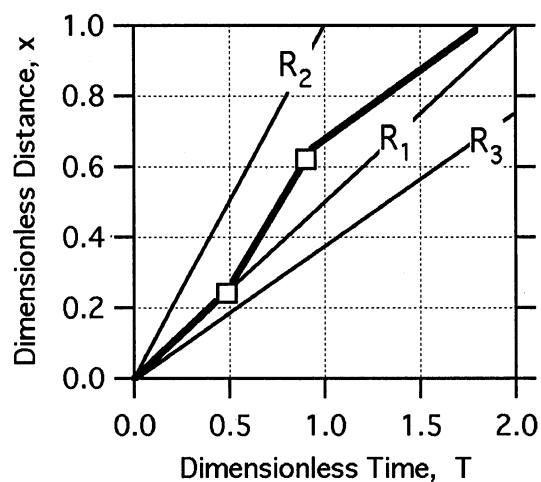


Figure 3-7 Effective trajectory of a particle that degrades sequentially from species 1 to species 3.

(considering plug flow and that each species has a different retardation coefficient  $R$ . Particle trajectory is shown in bold. Lighter lines are for nonreactive particles having same retardation coefficients of species 1, 2 and 3.)

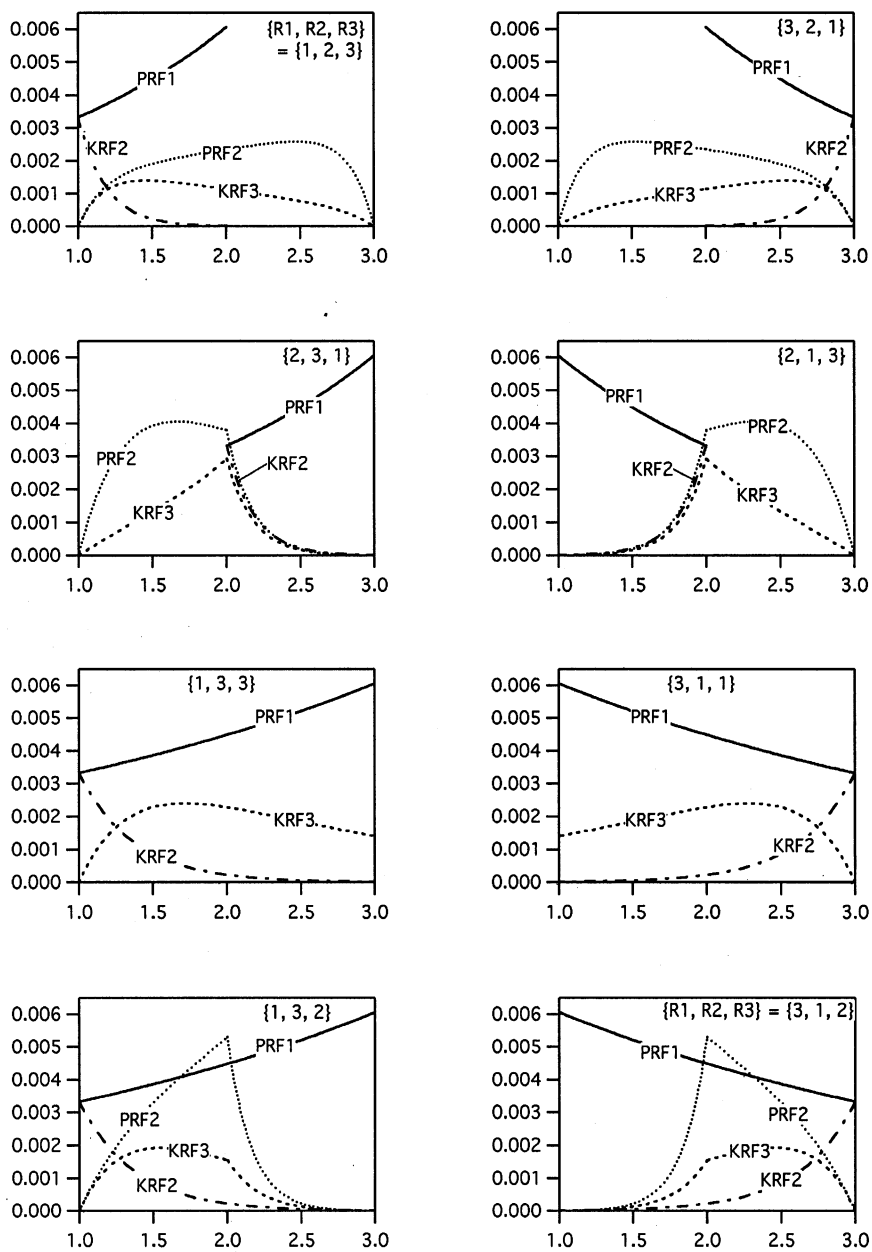


Figure 3-8 Product and Kinetic Response Functions (*PRF* and *KRF*) for three species.  
(in series plotted against dimensionless time at position  $x=1$ , for  $\{k_1, k_2, k_3\} = \{0.6, 6.0, 1.8\}$ .)

### 3.3.6 Kinetic Response Function Approach

The kinetic response function approach uses semi-analytical solutions of linear systems and works by de-coupling fluid transport processes (advection & dispersion) from reactivity and sorption processes. Straightforward, linear response functions are applied, rather than nonlinear constitutive transport equations. This approach extends the utility of common modeling programs for problems dealing with aquifer heterogeneity and complex reaction networks (Eykholt and Lin 2000). For the KRF method presented here, an analytical solution is used for the response functions in plug flow, then the kinetic residence time density or transfer function is generated directly from the numerical evaluation of the E-curve. The advantage is that a wide variety of mixing conditions and reaction networks may be considered without the need to generate analytical transfer functions for each species and mixing condition. The kinetic response function is developed for each species affected by adsorption and chemical reaction. Then, a residence time density function is applied to generate the kinetic E-curve. Effluent concentrations can be predicted from the convolution of the kinetic E-curve and input concentrations. The KRF approach is used here to study multiple species reactive transport in a heterogeneous aquifer. The objective of this study is to test the approach with regard to its accuracy and efficiency compared to other numerical packages.

### 3.3.7 RT3D

RT3D (Reactive Transport in 3 Dimensions) is a FORTRAN 90-based model for simulating 3D multi-species, reactive transport in groundwater. This model is based on the 1997 version of MT3D (DOD Version 1.5), but has several extended reaction capabilities. RT3D can accommodate multiple sorbed and aqueous phase species with several pre-defined reactions. It includes seven reaction packages including hydrocarbon biodegradation, non-equilibrium sorption, dual porosity model, and reductive, anaerobic biodegradation. It has been used to model groundwater remediation and natural attenuation (Clement et al. 2000).

Overall, the main steps for this study are shown in Fig. 3-9.

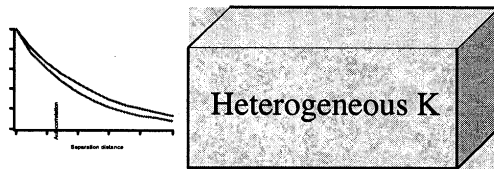
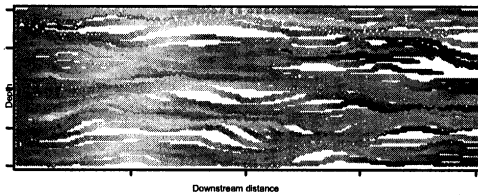
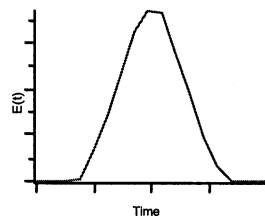
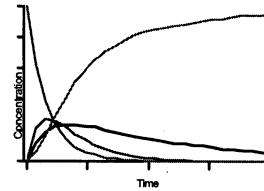
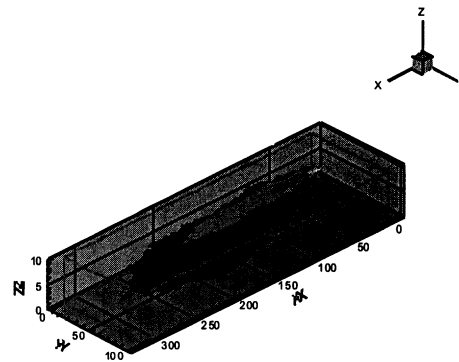
**STEP 1: Aquifer Generation****STEP 2: Flow & Particle Tracking****STEP 3:  $E(t,x,y,z)$  Generation****STEP 4: Reaction Mechanism Modeling****STEP 5: Concentration Estimates**

Figure 3-9 Steps for KRF approach used

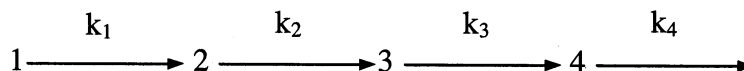
## 4. RESULTS AND DISCUSSION

In this part, the main numerical results from the KRF approach will be presented. For simple flow system, the KRF approach is verified by others analytical models such as provided by Sun (1999) and Van Genuchten (1985). For heterogeneous aquifers, the random fields of heterogeneous hydraulic conductivity will be generated with TBM method. For each reactive transport simulation of the KRF approach, RT3D is used for comparison and to verify the KRF approach.

### 4.1. Simple Flow System

A simple flow system means that residence time density function  $E(t)$  can be expressed analytically. For example, CSTR, N-CSTR, plug flow, and one-dimensional uniform flow with three-dimensional dispersion are mixing models that can be used to apply and check KRF solutions.

As shown in Fig. 4-1, the KRF method was compared to the analytical solution provided by the CHAIN model of van Genuchten (1985) for a four member decay chain with advective-dispersive flow (1<sup>st</sup> type boundary conditions). The reaction mechanism was considered:



Where,  $k_i$  is first order reaction constant rate of species  $i$ . Species 2 and 3 had the same retardation coefficient, but  $R_1$  and  $R_4$  were different. A high Peclet number was selected to test the ability of the method to predict arrival times from sharp fronts accurately. For the fourth species, the relative error at the peak concentration was 0.023%. However, for the first three species, the relative error was insignificant.

The KRF method was also verified with Sun *et al.* (1999) analytical solution for the advection-dispersion equation in 3D with a constant, rectangular, plane source. The analytical E-curve is shown in Eq.3.11. Four sequential first order decay species are considered. Results from one simulation are shown in Fig.4-2, revealing a suitable comparison with the Sun solution.

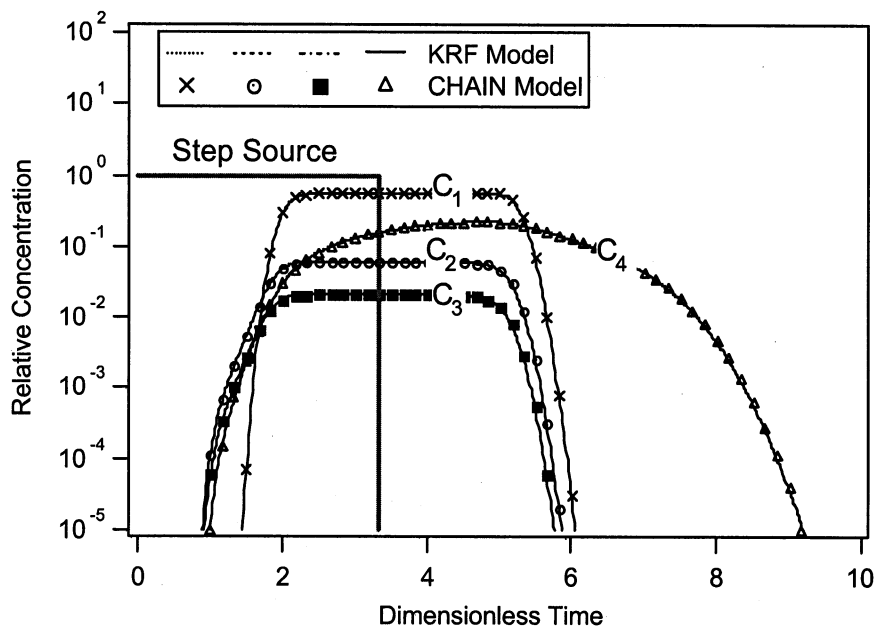


Figure 4-1 Verification of kinetic residence time density method through comparison of CHAIN analytical solution (van Genuchten 1985).

(Model run is for retardation coefficients  $R_i = \{2, 1, 1, 5\}$ , first order decay rate constant  $k_i = \{0.6, 6.0, 18., 1.2 \text{ day}^{-1}\}$ , residence time  $L/v = 60$  days, and Peclet number  $P = 333$ .)



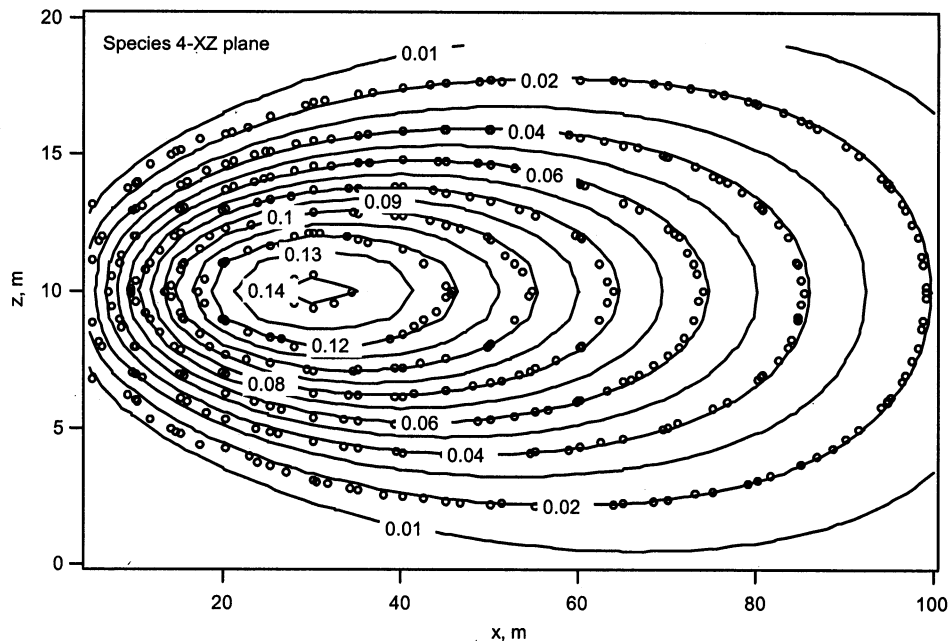


Figure 4-2 Plume simulation at  $t = 500$  d for 4<sup>th</sup> species in a decay chain resulting from rectangular, continuous source of the 1<sup>st</sup> species.

(Source dimensions  $Y_0 = 10$  m,  $Z_0 = 5$  m, centered at  $x = 0$  m,  $y = 20$  m. Dimensionless concentration from the KRF method (dots) compared with Sun *et al.* (1999) solution (smooth curves). Transport parameters are  $v=0.2$  m/day,  $D_x = 0.3$ ,  $D_y = 0.09$ , and  $D_z = 0.03$  m<sup>2</sup>/d. Retardation coefficients  $R_i = \{1, 1, 1, 1\}$ , first order decay rate constant  $k_i = \{0.05, 0.02, 0.01, 0.005 \text{ day}^{-1}\}$ .)

## 4.2. Complex Flow System

For a heterogeneous hydraulic conductivity field, the groundwater flow is complex and varies with site conditions. Multiple reactive species transport processes in a heterogeneous aquifer lead to even more complex results. In a remediation design scenario, numerical modeling is needed. In this study, the semi-analytical KRF approach can predict transient concentrations of multiple reactive species in heterogeneous aquifers.

### 4.2.1 Heterogeneous aquifer and numerical E-curve

For this case, more than ten sets of heterogeneous aquifers were generated with TBM to reflect two-dimensional, three-dimensional, unconfined or confined aquifers. The hydraulic conductivity was set to be distributed log-normally with a mean of ( $\mu_{\ln K}$ ) - 10.3 m/s, and standard deviation ( $\sigma_{\ln K}$ ) ranging from 0.2 to 2.0. All of the 3D aquifers were approximated by stacked, two-dimensional hydraulic conductivity fields, with the assumption that the correlation in z direction was less than the layer thickness of 0.5 m.

**Table 4-1 Cases of heterogeneous aquifers in this study**

Case	Represented size of aquifers (LxWxD), m	Grid space, m	Correlation length in x (m)	Correlation length in y (m)	$\mu_{\ln K}$ (m/s)	$\sigma_{\ln K}$
2D	80 x 40	1	3	2	-10.3	0.5, 1.5, 1.5, 2.0
	8 x 8	0.1	6	3	-10.3	0.5, 1.5, 1.5, 2.0
	80 x 40	0.5	3	1	-10.3	0.5, 1.5, 1.5, 2.0
	480 x 240	3	3	2	-10.3	0.5, 1.5, 1.5, 2.0
	480 x 240	3	9	8	-10.3	0.5, 1.5, 1.5, 2.0
3D	15 x 9 x 2.5	0.1	10	5	-10.3	0.5, 1.5, 1.5, 2.0
	86 x 65 x 10	0.288	10	5	-10.3	0.5, 1.5, 1.5, 2.0
	320 x 100 x 10	2	5	4	-10.3	0.5, 1.5, 1.5, 2.0

#### 4.2.2.1 Numerical E-curve from the modified Path3D

As described in Eq.3.14, a numerical E-curve can be estimated for a heterogeneous aquifer with steady-state groundwater flow. A portion of a heterogeneous aquifer within a length of 480 m and width of 240 m was modeled in 2D with a uniform grid spacing of 3 m. A log-mean hydraulic conductivity of -10 m/s was assumed with log-standard deviations ( $\sigma_{\ln K}$ ) of 1.0. Correlation lengths were selected to be  $\lambda_x = 3$  m,  $\lambda_y = 2$  m. Constant head boundaries were applied at the east and west sides to provide a horizontal hydraulic gradient of 0.01. Effective porosity was 0.3. 99 particles were released instantaneously at the cell of column 60 and row 41. Fig.4-3a is particle tracking path from the Path3D. Fig.4-3b is the numerical E-curve found from the particle tracking results at the receptor at column 90 and row 41. Particle tracking results for the heterogeneous aquifer clearly show an irregular flow path. After leaving the source cell,

the particles follow the main flow toward the east side, but they may move North or South to follow the preferential flow regions of higher conductivity. The numerical E-curve is shown in Fig. 4-3b. The peak of the  $E(t)$  has the highest residence time density, i.e., most of the particles pass the receptor at the time. The long tailing shows that the heterogeneous flow causes some particles to spend more residence time than others. The noise in the  $E(t)$  results from counting discrete particles, without any smoothing or weighting.

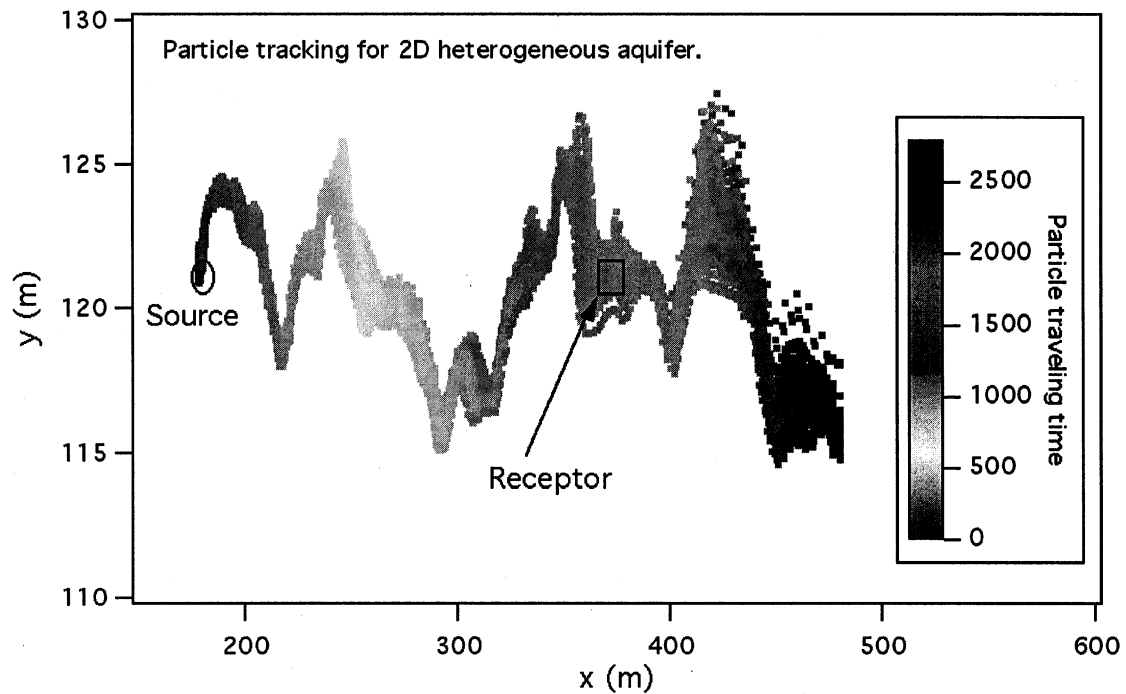


Figure 4-3a Particle tracking path in a 2D heterogeneous aquifer.

(The aquifer has 480 m length, 240 m width, 3 m uniform grid spacing,  $\mu_{lnK} = -10$ (m/s),  $\sigma_{lnK} = 1.0$ ,  $\lambda_x = 3$  m,  $\lambda_y = 2$  m,  $n = 0.3$ . 99 particles were instantaneous released at cell of column 60 and row 41.)

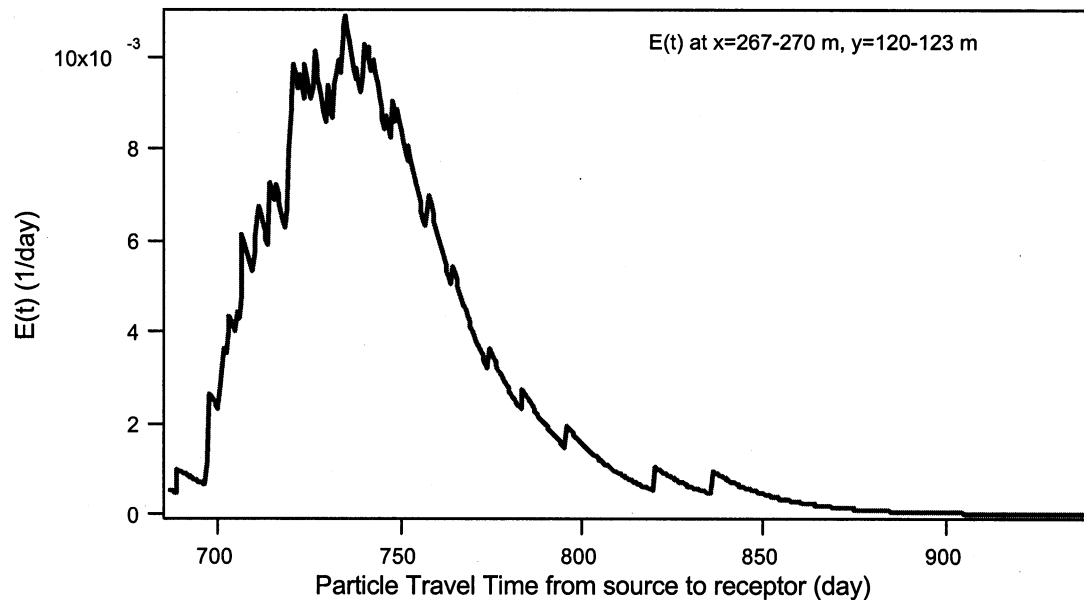


Figure 4-3b Numerical E-curve at receptor located at cell of column 90 and row 41.

In order to verify the E-curve method from modified Path3D, a hypothetical aquifer was used to compare the relative concentration from MT3D and the modified Path3D. The aquifer includes five impermeable units (walls). Hydraulic conductivity in the aquifer is assumed as 1 m/day. The horizontal hydraulic gradient 0.1 was applied to provide a flow from west to east. Effective porosity was 0.4. A 10 m length of strip-source with 100 ppb source concentration was added at the west boundary. 900 particles are released in the source, and the particle-tracking path was captured by the modified Path3D, as shown in Fig.4-4a. The E-curve method can predict conservative species concentration, compared with MT3D. The results are shown in Fig. 4-4b. The comparisons of the two methods give reasonable match.

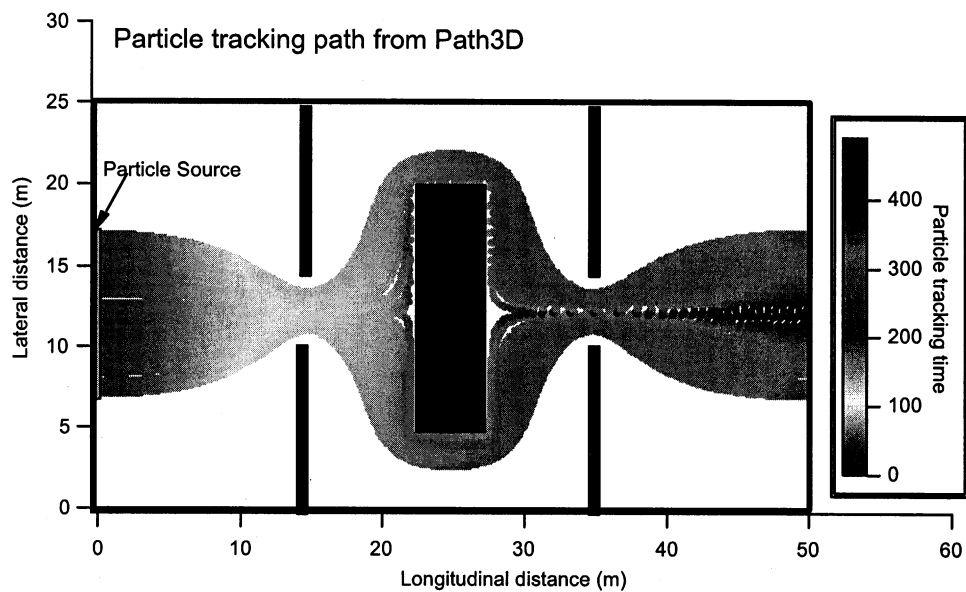


Figure 4-4a Particle travel time in the hypothetical aquifer

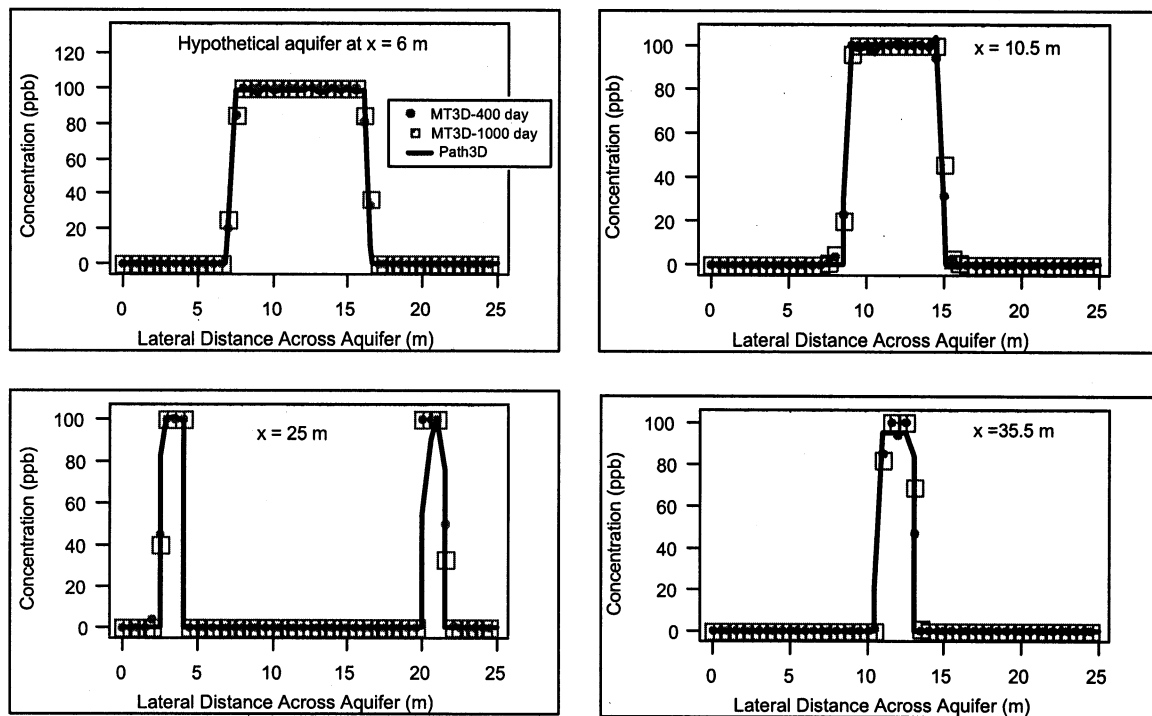


Figure 4-4b Compared with MT3D in the hypothetical aquifer

Fig.4-5 shows the comparison of MT3D and Path3D in four sections profiles in a 2D heterogeneous aquifer. Agreement of the two methods decreases as flow direction. The noise in the Path3D results may come from current particle counting method. Mass-conservative smoothing techniques may need to be developed for the method. In order to reflect numerical E-curve, MT3D method will be used.

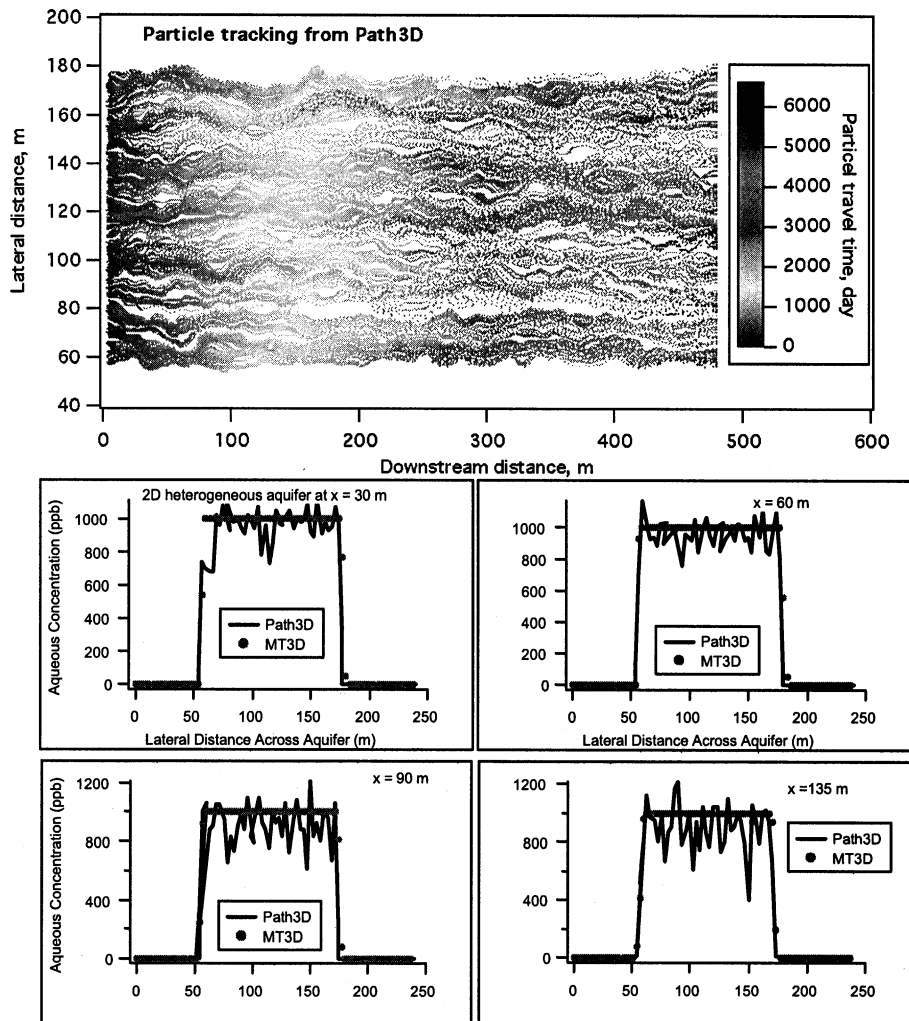


Figure 4-5 Compared with MT3D in the heterogeneous aquifer.

(The aquifer has 480 m length, 240 m width, 3 m uniform grid spacing,  $\mu_{lnK} = -10$  m/s,  $\sigma_{lnK} = 1.0$ ,  $\lambda_x = 3$  m,  $\lambda_y = 2$  m,  $n = 0.3$ . 99 particles were instantaneous released at line source.)

#### 4.2.2.2 Numerical E-curve from the MT3D

Using a conservative tracer test, an inert species is released at a continuous, constant source at the upstream, and MT3D is used to simulate the solute transport with advection and dispersion. We assume that the tracer does not sorb to the porous medium. Based on breakthrough curve at any location from MT3D solute transport result, analytical E-curve expression can be numerical calculated from the fitting Ogata and Bank parameters (see Eq. 3.17 and Eq. 3.18). Fig.4-6 and Fig.4-7 shows the breakthrough curves of tracer test along row 41 and column 80, and corresponding numerical E-curves at each monitoring point. Those E-curves reflect mixing characteristics of conservative species from the source to the monitoring points in the heterogeneous aquifer, which provide the system's flow information to KRF approach for reactive transport modeling. The numerical E-curve method from MT3D tracer test has been tested in this study for different heterogeneity cases.

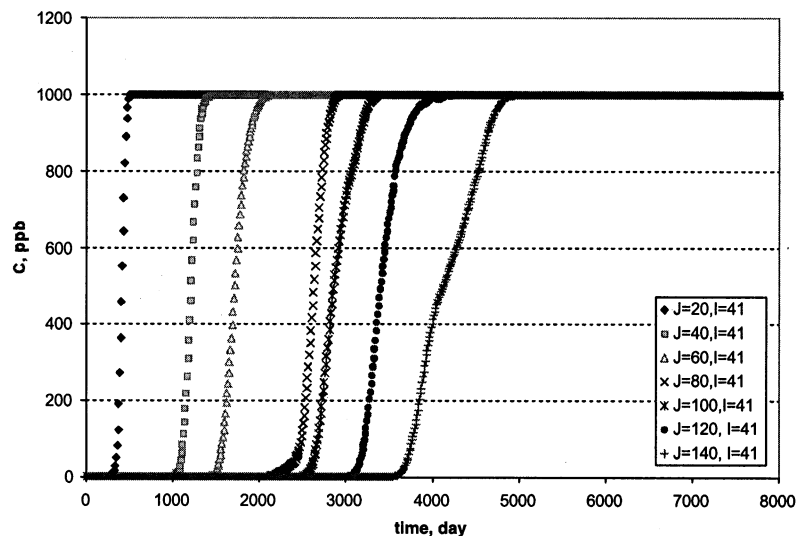


Figure 4-6a Tracer test along row 41 by MT3D in the heterogeneous aquifer.

(The aquifer has 480 m length, 240 m width, 3 m uniform grid spacing,  $\mu_{lnK} = -10$  m/s,  $\sigma_{lnK} = 0.5$ ,  $\lambda_x = 3$  m,  $\lambda_y = 2$  m,  $n = 0.3$ . Continuous line source of conservative species with 1000 ppb at the column 2<sup>nd</sup> and row 20 to 59.)

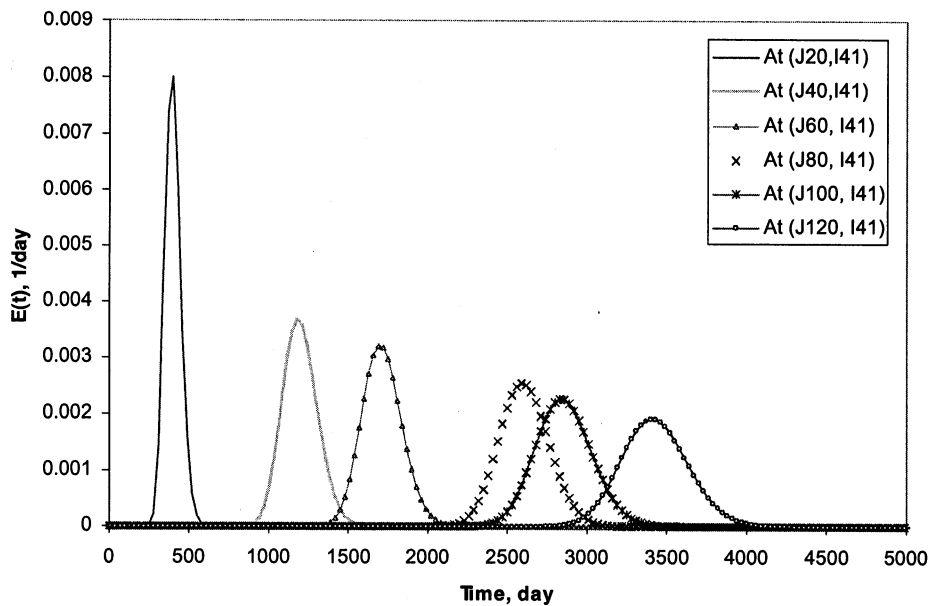


Figure 4-6b Numerical E-curve along row 41 from MT3D tracer test.

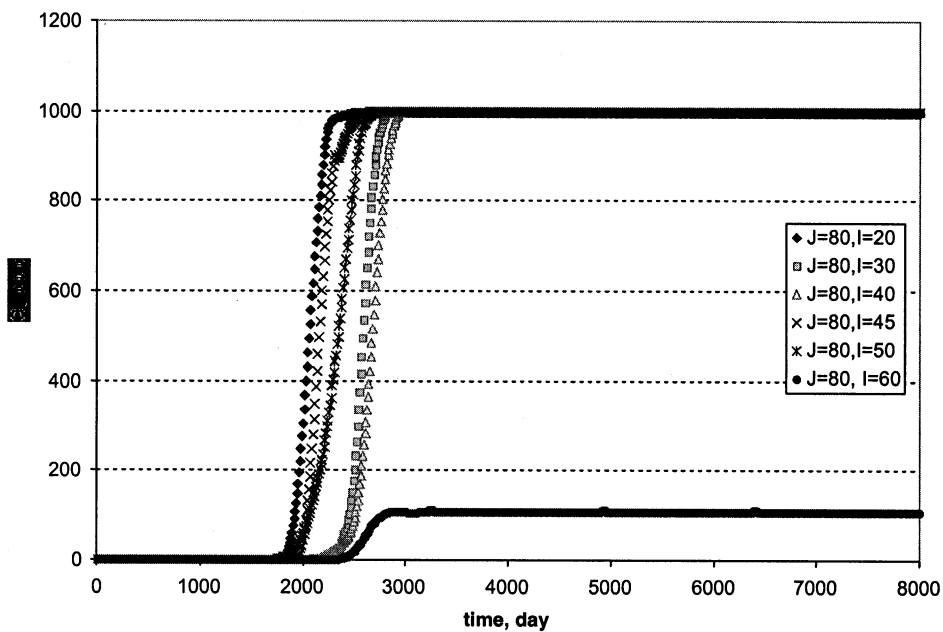


Figure 4-7a Tracer test along column 80 by MT3D in the heterogeneous aquifer.

(The aquifer has 480 m length, 240 m width, 3 m uniform grid spacing,  $\mu_{inK} = -10$  m/s,  $\sigma_{inK} = 0.5$ ,  $\lambda_x = 3$  m,  $\lambda_y = 2$  m,  $n = 0.3$ . Continuous line source of conservative species with 1000 ppb at the column 2<sup>nd</sup> and row 20<sup>th</sup> to 59<sup>th</sup>.)



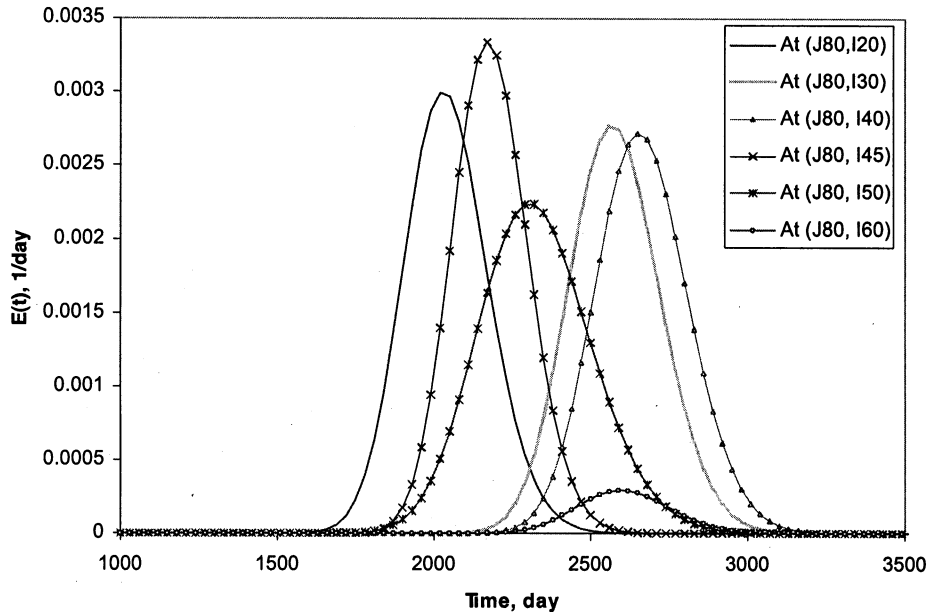


Figure 4-7b Numerical E-curve along column 80 from MT3D tracer test.

#### 4.2.2. Reactive transport simulation in heterogeneous aquifer

With the numerical E-curve generated by MT3D, the KRF approach can be applied to simulate reactive transport. Current analytical response functions are only available for sequential decay reactions up to 4 species, and reaction networks with up to 3 species. In this study, the KRF approach is mainly applied for prediction of 4 reactive species.

*Example 1:* A portion of a heterogeneous aquifer within a length of 480 m and width of 240 m was modeled in 2D with a uniform grid spacing of 3 m. A log-mean hydraulic conductivity of 1.1 m/day was assumed with log-standard deviations ( $\sigma_{\ln K}$ ) of 0.5. Correlation lengths were selected to be  $\lambda_x = 9$  m,  $\lambda_y = 8$  m. Constant head boundaries were applied at the east and west sides to provide a horizontal hydraulic gradient of 0.1. Effective porosity was 0.3. Longitudinal dispersivity was assumed as  $10^{-4}$  m, which only reflect molecular dispersion. 4 reactive species in sequential first order decay  $C1 \rightarrow C2 \rightarrow C3 \rightarrow C4 \rightarrow$  were selected with reaction rates of  $\{0.007, 0.005, 0.009, 0.001 \text{ day}^{-1}\}$ .

Different retardation factors of the four species were used {1.2, 1.1, 1.1, 1.5}. Continuous line source was only taken as 1000 ppb of C1.

Fig.4-8 shows the comparison of KRF method and RT3D results. The breakthrough curves of four species at one monitoring location are shown in each graph. The steady state concentrations and break through time from the KRF approach are well matched with RT3D solutions over those locations. The CPU time of the KRF approach is 300 times faster than RT3D. It shows that the new approach is computationally efficient.

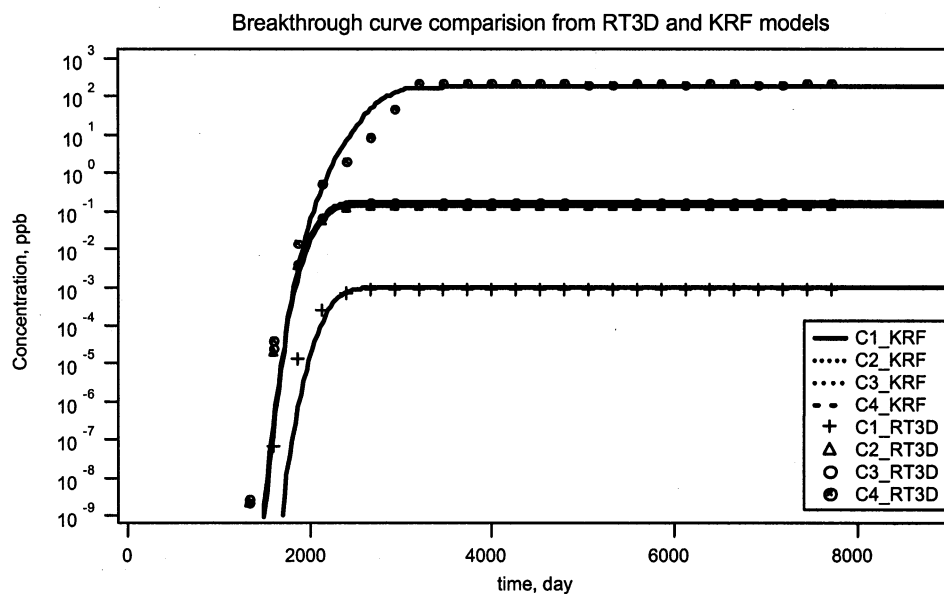


Figure 4-8a Comparison of the four species concentration with KRF approach and RT3D at monitoring point (row 20, column 80)

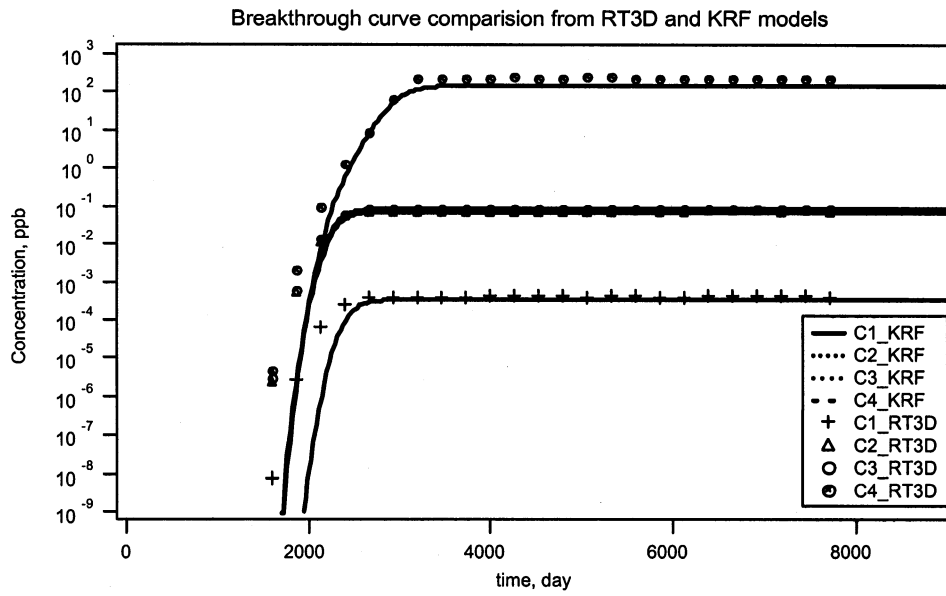


Figure 4-8b Comparison of the four species concentration with KRF approach and RT3D at monitoring point (row 45, column 80)

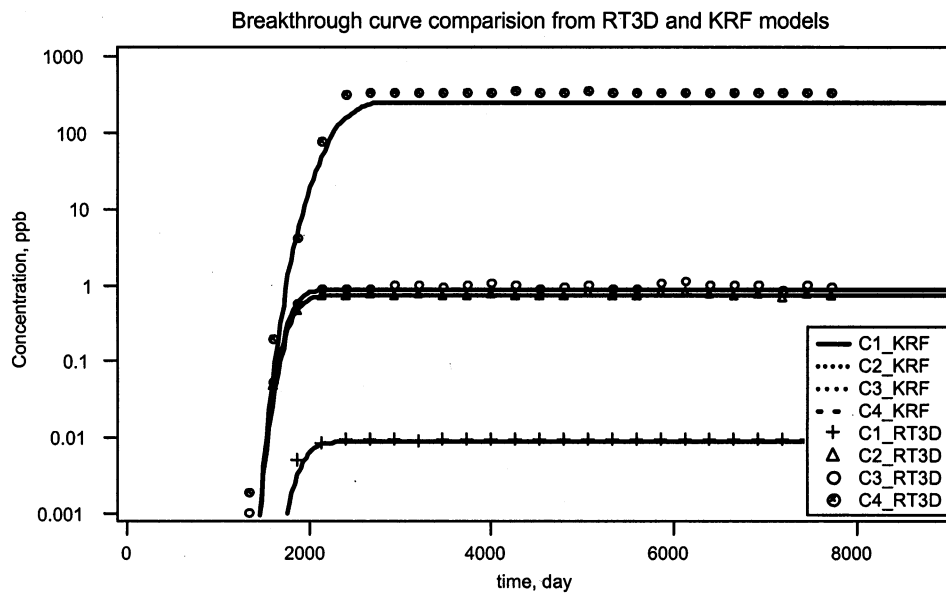


Figure 4-8c Comparison of the four species concentration with KRF approach and RT3D at monitoring point (row 41, column 60)

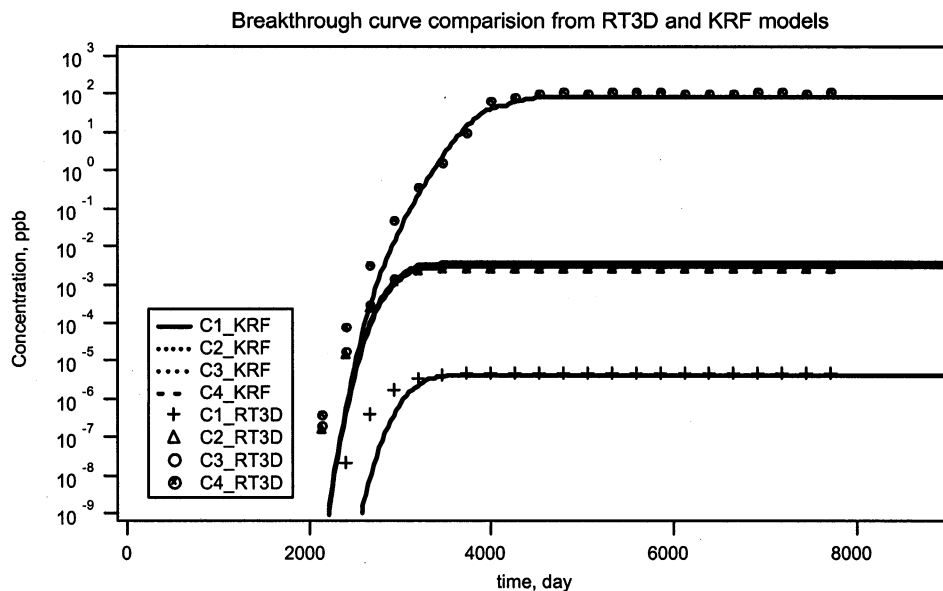


Figure 4-8d Comparison of the four species concentration with KRF approach and RT3D at monitoring point (row 41, column 100)

*Example 2:* A portion of a heterogeneous aquifer within a length of 480 m and width of 240 m was modeled in 2D with a uniform grid spacing of 3 m. A log-mean hydraulic conductivity of -10 m/s was assumed with log-standard deviations ( $\sigma_{\ln K}$ ) of 1.0. Correlation lengths were selected to be  $\lambda_x = 3$  m,  $\lambda_y = 2$  m. Constant head boundaries were applied at the east and west sides to provide a horizontal hydraulic gradient of 0.1. Effective porosity was 0.3. Dispersivity was assumed as 5 m in longitudinal direction and 0.5 m in transverse direction. 4 reactive species in sequential first order decay  $C1 \rightarrow C2 \rightarrow C3 \rightarrow C4 \rightarrow$  were selected with reaction rates of { of {0.006, 0.003, 0.01, 0.005 day<sup>-1</sup>}. Different retardation factors of the four species were used {1.8, 1.1, 1.1, 3.0}. Step line source was taken as 1000 ppb of C1 within first 83 days, then no source input after it.

Fig.4-9 shows the comparison of KRF method and RT3D results at three monitoring point. The breakthrough curves of four species predicted by the KRF approach are very

close to the RT3D results. But the KRF approach is 1500 times faster than the RT3D methods.

Table 4-2 shows the comparison of CPU time of the KRF approach and the RT3D model. The machine is Pentium III 600 MHz PC. This comparison is only limited to a 2D heterogeneous aquifer. The KRF approach is faster than RT3D from 160 times to 1440 times. It can be estimated the time difference will be greater in 3D case.

**Table 4-2 Comparison of run time between RT3D and KRF**

<b>Comparison case:</b>	<b>RT3D-CPU time</b>	<b>KRF-CPU time</b>	<b>Times (RT3D/KRF)</b>
Case 1: Continuous line source, 4 species with same retardation coefficient $R_i = 1$ , and first order reaction rate constant $k_i = \{0.01, 0.002, 0.02, 0.005 \text{ day}^{-1}\}$	2 hr	1 min	160
Case 2: Step line source with 67 days, 4 species with $R_i = 1$ , $k_i = \{0.001, 0.002, 0.02, 0.005 \text{ day}^{-1}\}$ . Dispersivity coefficient is 5 m in x and 0.5 m in y direction. Hydraulic gradient is 0.1.	5 hr	1 min	300
Case 3: Step line source with 83 days, 4 species with different retardation coefficient $R_i = \{1.8, 1.1, 1.1, 3.0\}$ , $k_i = \{0.001, 0.002, 0.02, 0.005 \text{ day}^{-1}\}$ . Dispersivity coefficient is 5 m in x and 0.5 m in y direction. Hydraulic gradient is 0.1.	24 hr	1 min	1440

As summary, the KRF approach applies analytical kinetic response function and numerical E curve to predict reactive transport of multiple species in heterogeneous aquifer. The numerical E-curve is simulated by MT3D. The KRF approach can compare with RT3D in the prediction accuracy and speed. Under the same accuracy with RT3D, the KRF approach shows a more computationally efficient reactive transport modeling method.

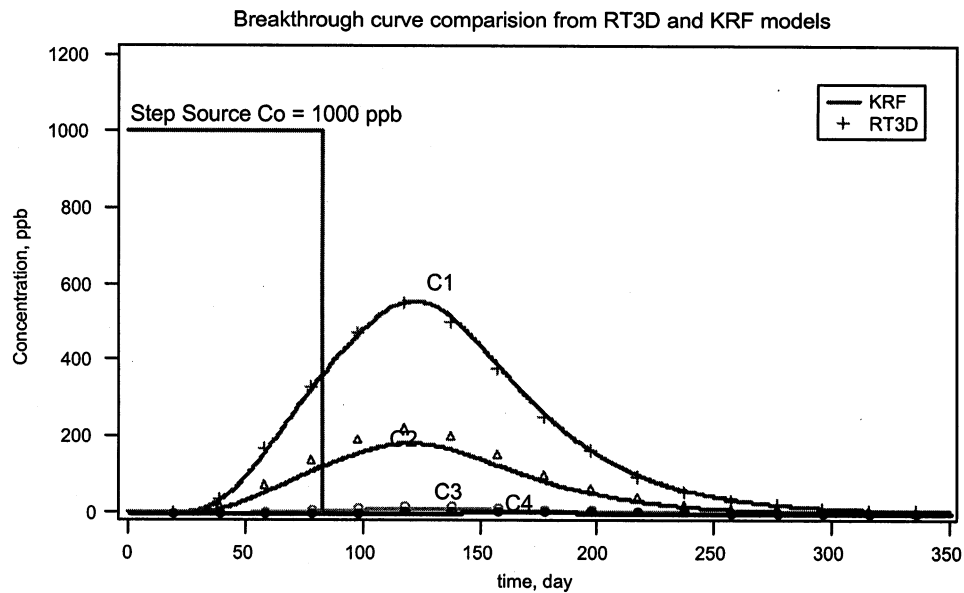


Figure 4-9a Comparison of the four species concentration with KRF approach and RT3D at monitoring point (row 41, column 20)

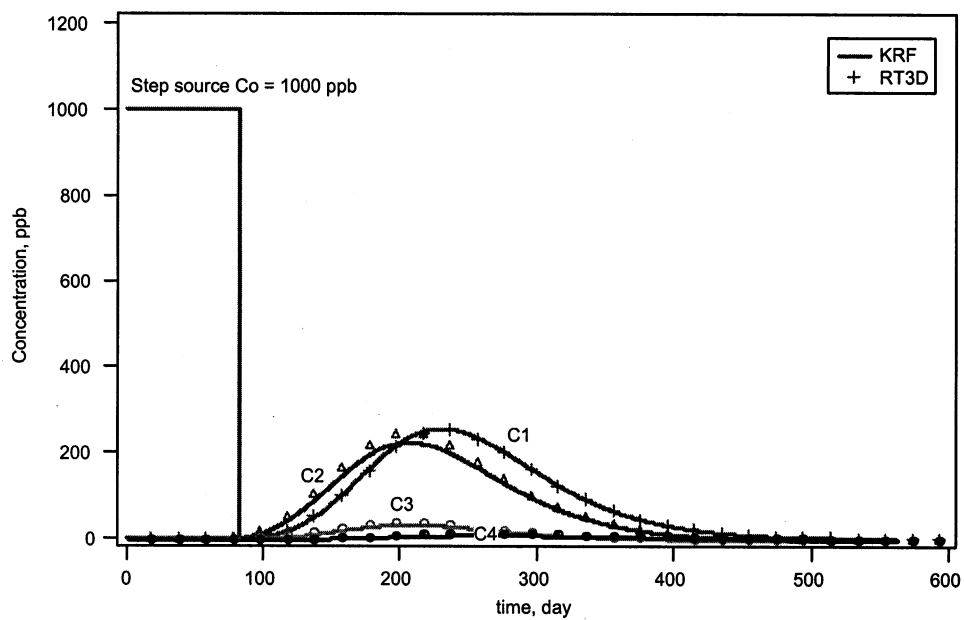


Figure 4-9b Comparison of the four species concentration with KRF approach and RT3D at monitoring point (row 41, column 40)

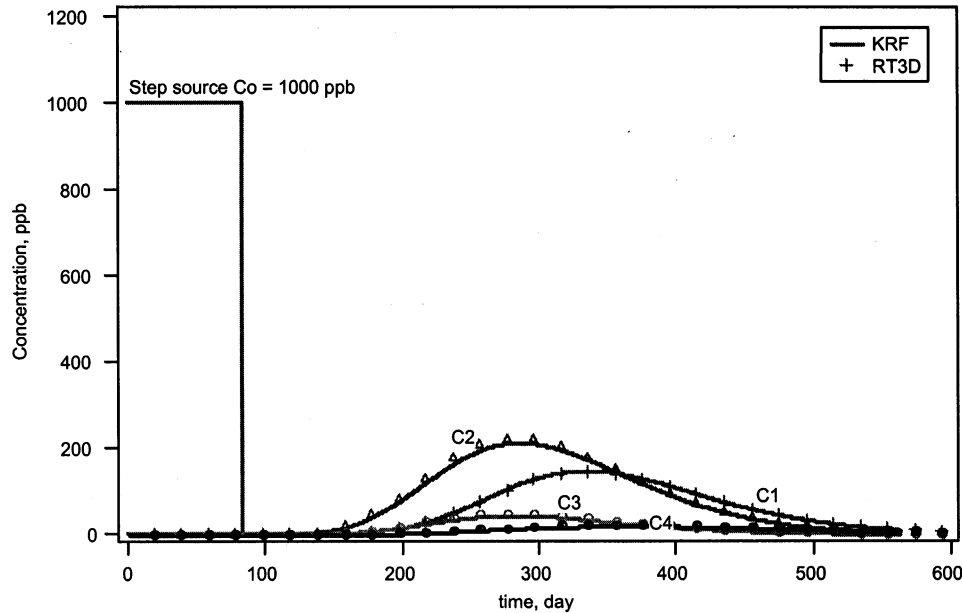


Figure 4-9c Comparison of the four species concentration with KRF approach and RT3D at monitoring point (row 40, column 60)

### 4.3. Sensitivity Analysis

In order to compare the KRF approach with RT3D model under different parameters, parameter sensitivity analysis were conducted. The parameters include mean of log-normal hydraulic conductivity ( $\mu_{\ln K}$ ), standard deviation of log-normal hydraulic conductivity ( $\sigma_{\ln K}$ ), correlation length ( $\lambda_x$ ,  $\lambda_y$ ), retardation coefficients  $R_i$ , and first order reaction rate constants  $k_i$ .

#### 4.3.1. Mean of log-normal hydraulic conductivity

Under the typical heterogeneous aquifer in above Example 1, the log-standard deviations ( $\sigma_{\ln K}$ ) was taken as 1.0. Correlation lengths were selected to be  $\lambda_x = 9$  m,  $\lambda_y = 8$  m. Constant head boundaries were applied at the east and west sides to provide a horizontal hydraulic gradient of 0.1. 4 reactive species in sequential first order decay  $C1 \rightarrow C2 \rightarrow C3 \rightarrow C4 \rightarrow$  were selected with reaction rates of  $\{0.007, 0.005, 0.009, 0.001 \text{ day}^{-1}\}$ . Different retardation factors of the four species were used  $\{1.2, 1.1, 1.1, 1.5\}$ . Continuous line source was only taken as 1000 ppb of C1.

The log-mean hydraulic conductivity  $\mu_{\ln K}$  was tested as 0.2 m/day (or  $\mu_K = 2.3 \times 10^{-5}$  m/s), 1.1 m/day (or  $\mu_K = 5.7 \times 10^{-5}$  m/s), and 1.8 m/day (or  $\mu_K = 1.2 \times 10^{-4}$  m/s).

As mean of hydraulic conductivity increases, the aquifer has faster groundwater mean flow under same hydraulic gradient, and the residence time density function breaks early and narrows (Fig.4-10a). The KRF approach and RT3D model were used to predict the four species reactive transport in the aquifers. The difference between the two model was represented as RMS. It was taken from relative concentration difference of the 4<sup>th</sup> species. As shown in Fig.4-10b, the RMS difference varies from 0.01 to 0.016 as one order of magnitude of the mean hydraulic conductivity changing. It means that the KRF model has reasonable prediction results as RT3D does under different hydraulic conductivity field.

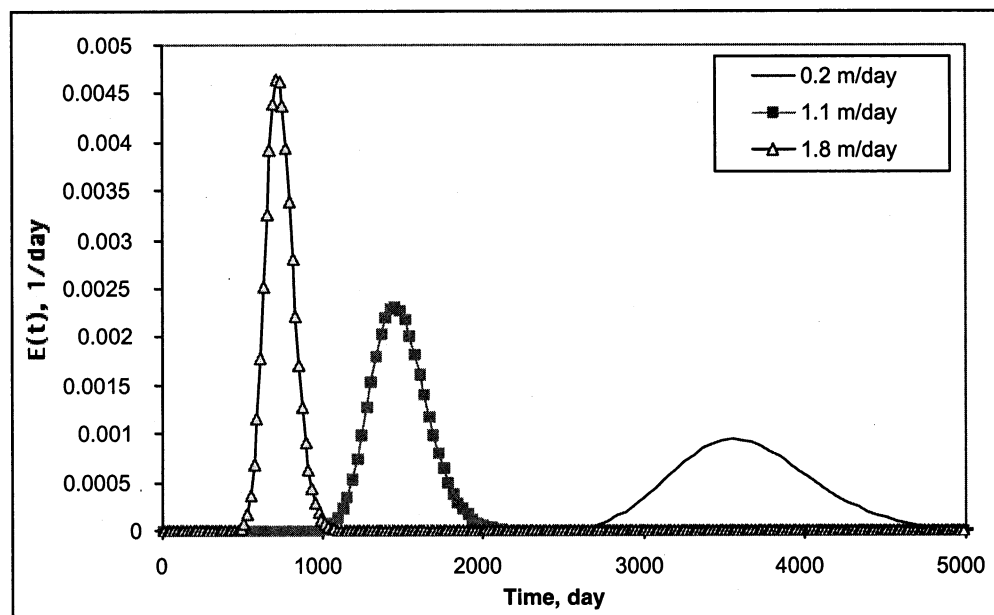


Figure 4-10a Numerical E curve under different mean of log-normal hydraulic conductivity at the row 41, and column 60.



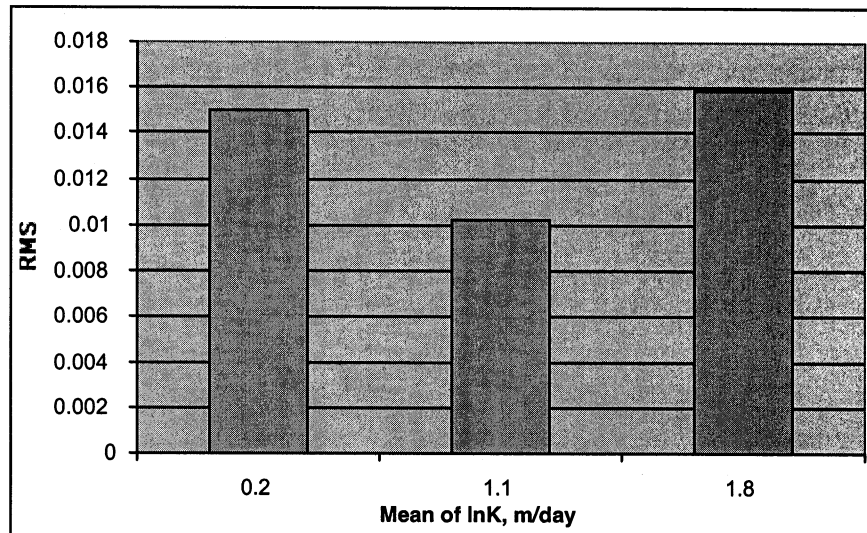


Figure 4-10b RMS of the 4<sup>th</sup> species between KRF model and RT3D model results under different mean of log-normal hydraulic conductivity

#### 4.3.2. Standard deviation of log-normal hydraulic conductivity

The log-mean hydraulic conductivity  $\mu_{\ln K}$  was fixed as 1.1 m/day (or  $\mu_K = 5.7 \times 10^{-5}$  m/s). The log-standard deviations  $\sigma_{\ln K}$  was tested at values of 0.2, 0.5 (nearly homogeneous aquifer), 1.0 and 1.5 (moderately heterogeneous aquifer).

As heterogeneity of hydraulic conductivity increases, the residence time density function tends to more board and late, as shown in Fig. 4-11a. Compared the KRF approach results with the RT3D, the RMS difference ranges from 0.005 to 0.01 for the 4<sup>th</sup> species (Fig.4-11b). It proves the accuracy of KRF approach under different heterogeneity. The sensitivity analysis of  $\mu_{\ln K}$  and  $\sigma_{\ln K}$  shows that the difference of KRF results and RT3D results are not sensitive to the two parameters, i.e., the KRF approach can make same reactive transport prediction as RT3D.

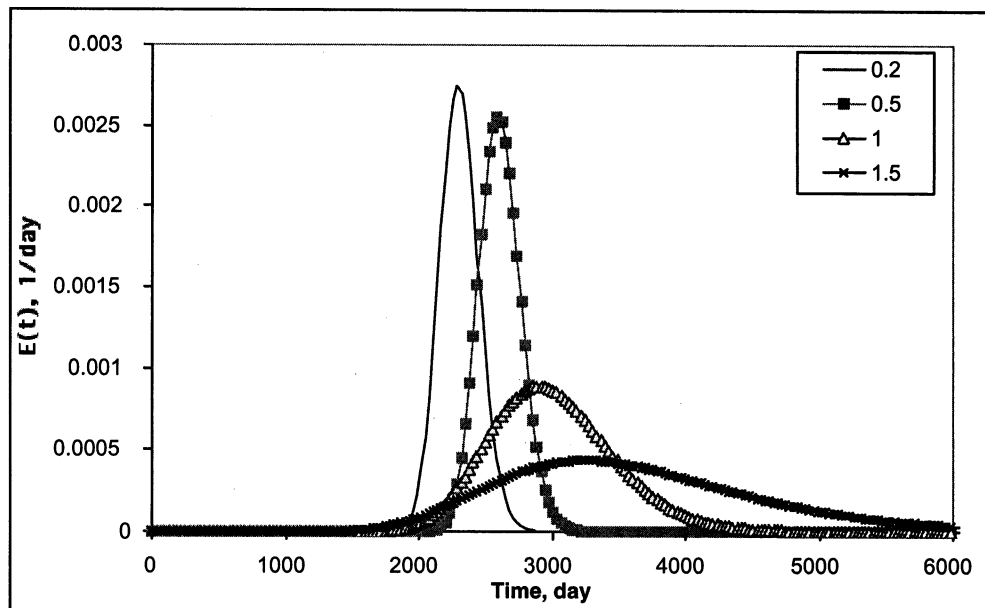


Figure 4-11a Numerical E curve under different standard deviation of log-normal hydraulic conductivity at the row 41, and column 80.

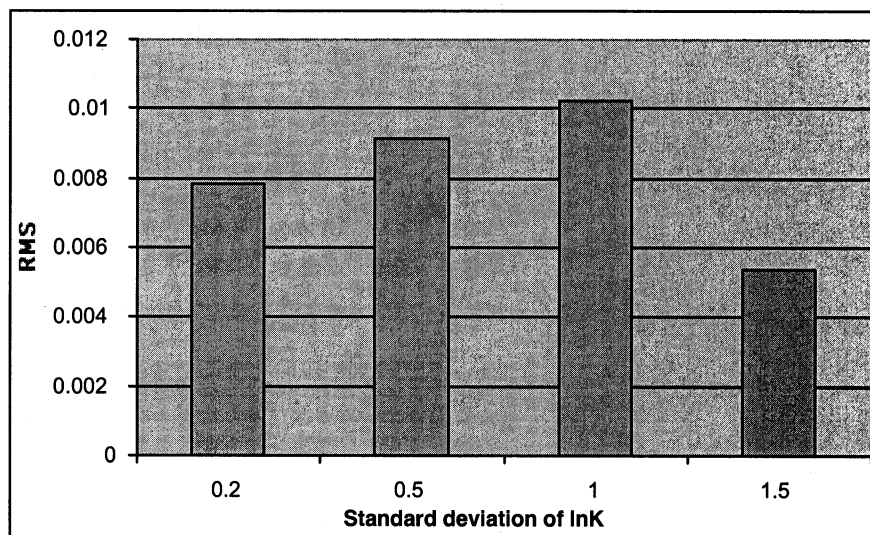


Figure 4-11b RMS of the 4<sup>th</sup> species between KRF model and RT3D model results under different standard deviation of log-normal hydraulic conductivity

### 4.3.3. Reaction parameters

In the KRF model, the reaction parameters include retardation coefficients and first order reaction rate constants. Because those reaction parameters are expressed through analytical kinetic response function under plug flow, the solution is accuracy under simple flow system. For the complex flow system, the results of KRF model depends on numerical E-curve quality. If the numerical  $E(t)$  can express the mixing characteristics of the flow system, the KRF approach also be able to accuracy predict the multiple reactive transport in the flow system. In Eykholt and Lin (2000) work, different reaction parameters have been tested to the prediction of KRF approach in simple flow system. In this study, the various reaction parameters have been tested to compare the RMS of KRF and RT3D solutions. As shown in Table 4-3, the RMS ranges from  $10^{-5}$  to  $10^{-2}$  as retardation coefficients and first order reaction rate constants changing. The low RMS shows that the KRF approach is not sensitive to vary reaction parameters and always predict reasonable matched results with RT3D model.

**Table 4-3 RMS difference in various reaction parameters**

Reaction parameters	RMS
$R_i = 1, k_i = \{0.01, 0.002, 0.02, 0.005 \text{ day}^{-1}\}$	0.001
$R_i = 1, k_i = \{0.001, 0.002, 0.02, 0.005 \text{ day}^{-1}\}$	$1 \times 10^{-3}$
$R_i = \{1.8, 1, 1, 1.1, 3.0\}, k_i = \{0.006, 0.003, 0.01, 0.005 \text{ day}^{-1}\}$	$4.1 \times 10^{-5}$
$R_i = \{1.2, 1.1, 1.1, 1.5\}, k_i = \{0.007, 0.005, 0.009, 0.001 \text{ day}^{-1}\}$	0.01

## 5. SUMMARY

In this study, a new modeling approach is developed for multiple reactive transport in heterogeneous aquifer. It can handle complex flow and reaction networks. The hypothesis of this work is that, for some problems, reactive transport in heterogeneous aquifers can be modeled with a linear method - where reactivity and flow distributions are not coupled.

The main idea of the approach is that, if the residence time density function  $E(t)$  of the system can be given, and the kinetic response function of each species be analytical described, prediction of transient species concentration are very straightforward with convolution technique at any location. Here, the system  $E(t)$  is assumed to be independent on the kinetic response function KRF of each species, i.e., the flow distributions and reactivity are not coupled in the heterogeneous aquifer. For simple flow system, the analytical residence time density function can be developed. For complex flow system, the residence time density  $E(t)$  can be numerical expressed. In this work, the definition of particle tracking techniques from Path3D is developed and applied into the numerical expression of system  $E$  curve. Although the  $E$  curve has some extent of noise, it still reflects the system flow mixing characteristics. At the same time, MT3D is also used in this work to simulate numerical  $E$  curve at the heterogeneous aquifer. For sequential first order reactions, analytical kinetic response function have been developed in previous works, and applied in this work to predict the transient concentration profile with time.

Several heterogeneous aquifers have been generated with turning band methods, and four species reactive transport simulations have been tested with the KRF approach developed in this study. From the numerical results, the KRF approach results are comparable with RT3D results. The computational CPU time comparison shows that the KRF approach is a high efficient method. From the numerical test, the hypothesis of this study is correct.

For heterogeneous hydraulic conductivity and homogeneous reaction rate, it is reasonable to uncouple the reactive transport into flow and reaction. It can decrease the simulation time and ensure an acceptable level of accuracy.

However, as stated in the above, the KRF approach is a semi-analytical method. It has some limitations. One is that it is only suitable for homogeneous reactions rate. The reason is that the kinetic response function for the reaction networks is developed analytically. It limits the application of the approach into heterogeneous reaction case. Another limitation of this method is that it can not provide the whole domain solution. It only gives the transient concentration at the monitoring points. When the method is integrated into modeling platforms (such as Groundwater Modeling System -GMS, Groundwater Vista's , etc), the limitations may be overcome.

## REFERENCES

- Arnold, W. and Roberts, A. (1998), "Pathways of chlorinated ethene and chlorinated acetylene reaction with Zn(0)", *Environmental Science and Technology*, 32(19): 3017-3025.
- Anderson, M.P (1997), "Characterization of geological heterogeneity", *Subsurface Flow and Transport: A Stochastic Approach*, edited by Dagan, G and Neuman, S.P., Cambridge University Press, 23-43.
- Charbeneau, R.J. (2000) *Groundwater Hydraulics and Pollutant Transport*. Prentice Hall, New Jersey.
- Cirpka, O.A. and Kitanidis, P.K. (2000), "An advective-dispersive stream tube approach for the transfer of conservative-tracer data to reactive transport", *Water Resources Research*, 36(5): 1209-1220.
- Clement, T.P (1997), "A modular computer model for simulating reactive multi-species transport in three-dimensional groundwater systems", *Pacific Northwest National Laboratory Report*, Richland, Washington, PNNL-SA-28967.
- Clement, T.P., Johnson, C.D, Sun, Y., Klecka, G.M. and Bartlett, C. (2000), "Natural attenuation of chlorinated ethene compounds: model development and field-scale application at the Dover site", *Journal of Contaminant Hydrology*, 42: 113-140.
- Danckwerts, P.V., (1953) Continuous flow systems. Distribution of residence time. *J. Chemical Engineering Science*, 2, 1.
- Elder, C. (2000), "Evaluation and Design of Permeable Reactive Barriers Amidst Heterogeneity", Ph.D. Dissertation, Department of Civil and Environmental Engineering, University of Wisconsin-Madison.
- Eykholt, G.R. (1999), "Analytical solution for networks of irreversible first-order reactions", *Water Research*, 33(3): 814-826.
- Eykholt, G.R., Elder, C.R. and Benson, C.H. (1999), "Effects of aquifer heterogeneity and reaction mechanism uncertainty on a reactive barrier", *Journal of Hazardous Materials*, 68(1/2): 73-96.
- Eykholt, G.R., and Lin Li (2000), "Fate and transport of species in a linear reaction network with different retardation coefficients", *Journal of Contaminant Hydrology*, 46: 163-185.
- Fenton, G. (1994), "Error evaluation of three random field generators", *Journal of Engineering Mechanics*, 120 (12): 2478-2497.
- Freeze, R. (1975), "A stochastic-conceptual analysis of one-dimensional groundwater flow in nonuniform homogeneous media", *Water Resources Research*, 11(5): 725-741.
- Gelhar, L. (1993), *Stochastic Subsurface Hydrogeology*, Prentice hall, Englewood Cliffs, New Jersey.

- Ginn, T.R. (2001), "Stochastic-convective transport with nonlinear reactions and mixing: finite streamtube ensemble formulation for multicomponent reaction systems with intra-streamtube dispersion", *Journal of Contaminant Hydrology*, 47: 1-28.
- Levenspiel, O. (1972) *Chemical Reaction Engineering*, Chap.9, John Wiley, New York.
- Mantoglou, A. and Wilson, J. (1982), "The turning bands method for simulation of random fields using line generation by a spectral method", *Water Resources Research*, 18(5): 1379-1394.
- McDonald, M. and Harbaugh, A.W. (1988), *MODFLOW, A modular three-dimensional finite-difference ground-water flow model*, U.S. Geological Survey.
- Nauman, E.B., (1981) Residence time distributions and micromixing, *Chem. Eng. Commun.*, 8: 53-131.
- Ogata, A. and Banks, R.B. (1961) A solution of the differential equation of longitudinal dispersion in porous media, *U.S. Geological Survey Professional Paper*, 411-I.
- Jury, W.A. (1982), "Simulation of solute transport using a transfer function model", *Water Resources Research*, 18(2): 363-368.
- Rainwater, K.A., Wise, W.R., and Charbeneau, R.J. (1987) Parameter estimation through groundwater tracer tests. *Water Resources Research*, 23 (10):1901-1910.
- Riemersma, P. (1996), "Geostatistical Characterization of Heterogeneity, Simulations of Advective Transport, and Evaluation of Pump-and-Treat Systems in Braided Stream Deposits", Ph.D. Dissertation, Department of Geology, University of Wisconsin-Madison.
- Roberts, A., Totten, L, Arnold, W., Burris, D., and Campbell, T. (1996), "Reductive elimination of chlorinated ethylenes by zero-valent metals", *Environmental Science and Technology*, 30(8): 2654-2659.
- Sun, Y. Petersen, J.N., Clement, T.P. (1999), "Analytical solutions for multiple species reactive transport in multiple dimensions", *Journal of Contaminant Hydrology*, 35: 429-440.
- Tompson, A., Ababou, R., and Gelhar, L. (1989), "Implementation of the three-dimensional turning bands random field generator", *Water Resources Research*, 25(10): 2227-2243.
- Yabusaki, S.B., Steefel, C.I. and Wood, B.D. (1998), "Multidimensional, multicomponent, subsurface reactive transport in nonuniform velocity fields: code verification using an advective reactive streamtube approach", *Journal of Contaminant Hydrology*, 42: 113-140.
- van Genuchten, M.Th., (1985), "Convective-dispersive transport of solutes involved in sequential first-order decay reactions", *Comput. Geosci.*, 11: 129-147.
- Webb, E. and Anderson, M. (1996), "Simulation of preferential flow in three-dimensional, heterogeneous conductivity fields with realistic internal architecture", *Water Resources Research*, 32(3): 533-545.

Zheng, C. (1991), *PATH3D 3.0: A ground-water path and travel-time simulator*, S.S.Papadopoulos & Associates, Inc., Bethesda, MD.

Zheng, C. (1992), *MT3D: A modular three-dimensional transport model for simulation of advection, dispersion and chemical reactions of contaminants in groundwater systems*, S.S.Papadopoulos & Associates, Inc., Bethesda, MD.